

Generalized perspective on chiral measurements without magnetic interactions

Andres F. Ordonez^{1,2,*} and Olga Smirnova^{1,2,†}

¹*Max-Born-Institut, Berlin, Germany*

²*Technische Universität Berlin, Berlin, Germany*

Abstract

We present a unified description of several methods of chiral discrimination based exclusively on electric-dipole interactions. It includes photoelectron circular dichroism (PECD), enantio-sensitive microwave spectroscopy (EMWS), photoexcitation circular dichroism (PXCD) and photoelectron-photoexcitation circular dichroism (PXECD). We show that, in spite of the fact that the physics underlying the appearance of a chiral response is very different in all these methods, the enantio-sensitive and dichroic observable in all cases has a unique form. It is a polar vector given by the product of (i) a molecular pseudoscalar and (ii) a field pseudovector specified by the configuration of the electric fields interacting with the isotropic ensemble of chiral molecules. The molecular pseudoscalar is a rotationally invariant property, which is composed from different molecule-specific vectors and in the simplest case is a triple product of such vectors. The key property that enables the chiral response is the non-coplanarity of the vectors forming such triple product. The key property that enables chiral detection without relying on the chirality of the electromagnetic fields is the vectorial nature of the enantio-sensitive observable. Our compact and general expression for this observable shows what ultimately determines the efficiency of the chiral signal and if, or when, it can reach 100%. We also discuss the differences between the two phenomena, which rely on the bound states, PXCD and EMWS, and the two phenomena using the continuum states, PECD and PXECD. Finally, we extend these methods to arbitrary polarizations of the electric fields used to induce and probe the chiral response.

* ordonez@mbi-berlin.de

† smirnova@mbi-berlin.de

I. INTRODUCTION

Right- and left-handed helices are typical examples of chiral objects; each of them cannot be superimposed on its own mirror image. Some molecules possess the same property; left-handed and right-handed molecules are called enantiomers. Distinguishing left and right enantiomers is both vital and difficult [1–3]. Since the XIX century, the helix of circularly polarized light was used to distinguish the two enantiomers of a chiral molecule, relying on the relatively weak interaction with the magnetic field as a key mechanism for chiral discrimination. However, in this case the chiral signal¹ is proportional to the ratio of the molecular size to the pitch of the light helix, i.e. its wavelength, generally leading to weak signals in the infrared, visible, and UV regions.

One can overcome this unfavorable scaling and obtain significantly higher circular dichroism, at the level of a few percent, in several ways. Firstly, one can rely on using a strong laser field to enhance the magnetic-dipole transitions and interfere them against the electric-dipole ones, as done in chiral high harmonic generation [4–7]. Secondly, one can decrease the pitch of the light helix by using XUV/X-ray light [8, 9]. Yet, in both cases the chiral signal would be equal to zero within the electric-dipole approximation.

Thus, the discovery of approaches relying exclusively on electronic dipole transitions [10–18] and yielding a very high chiral response already in the electric-dipole approximation is both intriguing and beneficial. These techniques include photoelectron circular dichroism (PECD) [10–13], enantio-sensitive microwave spectroscopy (EMWS) [16, 19, 20], photoexcitation circular dichroism (PXCD) [18], and photoexcitation-photoelectron circular dichroism (PXECD) [18].

¹ When referring to the measured signal, we will use the adjective *chiral* as a shorthand for *enantio-sensitive and dichroic*.

This new generation of chiral methods leads to very high signals, up to tens of percent in PECD, which is several orders of magnitude higher than in standard techniques relying on magnetic interactions. Here we present a unified description of several of these methods working in the perturbative one- and two-photon regimes of the light-molecule interaction. Results for the multiphoton [21–23] and the strong-field regime [24, 25] of PECD will be presented elsewhere.

We derive a common general formulation for the chiral response encompassing PECD, EMWS, PXCD, and PXECD. This formulation is based on understanding that these electric-dipole based techniques using non-chiral fields are only possible thanks to vectorial observables. Readers familiar with chiral measurements might be uncomfortable with such statement. Indeed, it is well known that chiral observables are pseudoscalars, not polar vectors. Section II addresses this issue and describes the role of the lab setup in enantio-sensitive techniques with non-chiral fields. In Sec. III we describe how symmetry enforces enantio-sensitivity and dichroism on polar vectors resulting from the electric-dipole interaction. Section IV consists of four parts which specify how the information about the handedness of the lab setup and that of the molecular enantiomer can be decoupled and defined in a common way for the four perturbative dipole techniques: PECD, PXCD, EMWS, and PXECD. Section V summarizes the conclusions of this work. We use atomic units throughout the paper.

II. CHIRAL MEASUREMENTS AND ENANTIO-SENSITIVE OBSERVABLES

The goal of our work is to demonstrate the general concept underlying several chiral measurements which do not use magnetic interactions. Achieving this goal requires

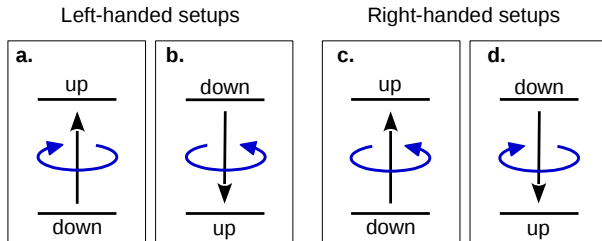


Figure 1. The combination of circularly polarized light (blue curved arrows) and a detector (horizontal lines) defining a vector perpendicular to the polarization plane (black vertical arrows) make up a chiral setup. Four possible realizations of such setup are shown. Setups **a** and **b** are left handed and setups **c** and **d** are right handed. For a fixed molecular enantiomer (not shown in the figure) setups with the same handedness yield the same result, while setups with opposite handedness yield opposite results.

two things. First, one should provide a general concept, i.e. address the question “*what is the key difference between the chiral measurements involving the magnetic component of the light field and those relying only on the electric-dipole approximation?*”. We outline such concept in this section. Second, one should formalize this concept by deriving compact expressions for observables pertinent to the four different experimental setups and establishing connections between them. Such derivations will be presented in Sec. [IV](#).

It is well known that any enantio-sensitive observable should be a pseudoscalar. However, detectors in any experimental setup measure clicks. Clicks are scalars. Where is the pseudoscalar in a click?

Let us start with the conventional concept. It is well known that the handedness of chiral objects can only be probed via interaction with another chiral object, in other words, it is well known that one always needs a chiral reagent to discriminate

between opposite enantiomers. A chiral reagent interacts differently with left and right enantiomers. The chiral reagent can be simply another chiral molecule or chiral light. Consider, for example, absorption circular dichroism. Absorption of circularly polarized light by a chiral molecule is the outcome of such an experiment, and this absorption must be different for right and left enantiomers. The difference in absorption is a scalar, however this scalar is just a product of two pseudoscalars, one from the molecule and the other from light. In this particular case the second pseudoscalar is the light helicity (see Appendix VII A), which encodes the handedness of the helix traced by the circularly polarized light in space. Thus, we use the chiral probe (chiral reagent) to “hide” a molecular pseudoscalar inside a scalar. The molecular pseudoscalar in absorption circular dichroism, as it is well known, is given by the scalar product of electric-dipole and magnetic-dipole vectors. The overall signal is small because the magnetic field interacts very weakly with molecules.

We now turn to methods which do not rely on the interaction with the magnetic component of the light field such as e.g. PECD. In PECD the photoionization of an isotropic molecular ensemble with circularly polarized light yields a net photoelectron current in the direction perpendicular to the plane of polarization. The direction of this current can be flipped by either swapping the molecular handedness or the direction of rotation of the field. It is a purely electric-dipole effect: light chirality is not needed at all, i.e. the magnetic field of the incident laser pulse is not used. Thus, we do not use the chiral property of light, yet the chiral signal is very strong. Where is our chiral reagent if the light chirality is not used? The combination of circularly polarized light and a detector that distinguishes the two opposite directions perpendicular to the polarization plane defines a chiral setup (see Fig. 1) whose handedness (a pseudoscalar) is given by the scalar product between the photon’s spin (a pseudovector) and the direction defined by the detector (a vector). Thus, the

chiral reagent is substituted by the chiral observer (i.e. chiral setup). That is why we do not need to employ chiral properties of impinging electromagnetic fields.

The role of the directionality of the detector in defining the handedness of the chiral setup highlights the crucial importance of having a vectorial response to the light-matter interaction, since a scalar response would be unable to exploit the directionality of the detector, and as a consequence also the handedness of the setup. Furthermore, as we show in Sec. III, such vectorial response automatically exhibits enantio-sensitivity and dichroism with respect to the *external* vector defined by the detector. These properties indicate that in general the vectorial response results from the product of a molecular pseudoscalar and a field pseudovector. The field pseudovector determines the direction of observation of the dichroic and enantio-sensitive response and thus indicates (up to a sign) the corresponding detector arrangement required to measure such response (see Fig. 1). The field pseudovector is formed by non-collinear (and phase-delayed in the case of a single frequency) components of the electric field. For example, in PECD, it results from the vector product between the x and y components of the circularly polarized field. Ultimately, the result of the measurement—the scalar (click)—is given by the projection of the vectorial response on the *external* vector defined by detector, which yields the product of the molecular pseudoscalar and the handedness of the setup (see Sec. IV). The latter is the projection (positive or negative) of the field pseudovector on the *external* vector defined by the detector.

Note that the field pseudovector does not have to point in the direction of light propagation (as one might think from the above example). In Sec. IV we expose various opportunities offered by different field geometries, including arrangements of electric fields propagating non-collinearly.

In Sec. IV we illustrate this concept by deriving molecular pseudoscalars and field

pseudovectors for four experiments detecting different observables in different systems using different setups. However, in all cases what enables chiral discrimination is the chiral observer defined by the combination of an achiral electromagnetic field and a directional detector.

III. SYMMETRY IN THE ELECTRIC-DIPOLE APPROXIMATION

Let us begin with a simple symmetry consideration, which applies to all enantio-sensitive effects considered here. Consider first an isotropic ensemble of a non-racemic mixture of chiral molecules, which interacts with light circularly polarized in the xy plane. Irrespective of the specific chiral response we are looking at, it may lead to an observable associated with some polar vector \vec{v} . For example, in the case of PECD this polar vector is the net photoelectron current, while in PXCD it would be the coherent dipole induced in the bound states of the neutral. The cylindrical symmetry of the “ensemble+field” system implies that $\vec{v} = v_z \hat{z}$ ². Generalization to the case with no cylindrical symmetry is discussed below. The “enantiomer+field” system and a chiral sensitive vectorial observable in the case of cylindrical symmetry are sketched in the upper-left box of Fig. 2. It applies, for example, to the field configuration in PECD and PXCD. Our system transforms as indicated in Fig. 2 under reflections in the xy plane and under rotations by π radians around any axis contained in the xy plane. These transformations show the relationship between the different “enantiomer+field” configurations and the corresponding effect on the dichroic and enantio-sensitive observable \vec{v} .

² Note that for few-cycle pulses, the cylindrical symmetry may be severely compromised. However, for perturbative fields the first-order amplitudes do not encode the duration of the pulse, that is, the response of a few-cycle pulse can be emulated using monochromatic light of the appropriate intensity, and therefore the cylindrical symmetry assumption remains valid even for ultra-short pulses provided one only looks at functions of the first-order amplitudes.

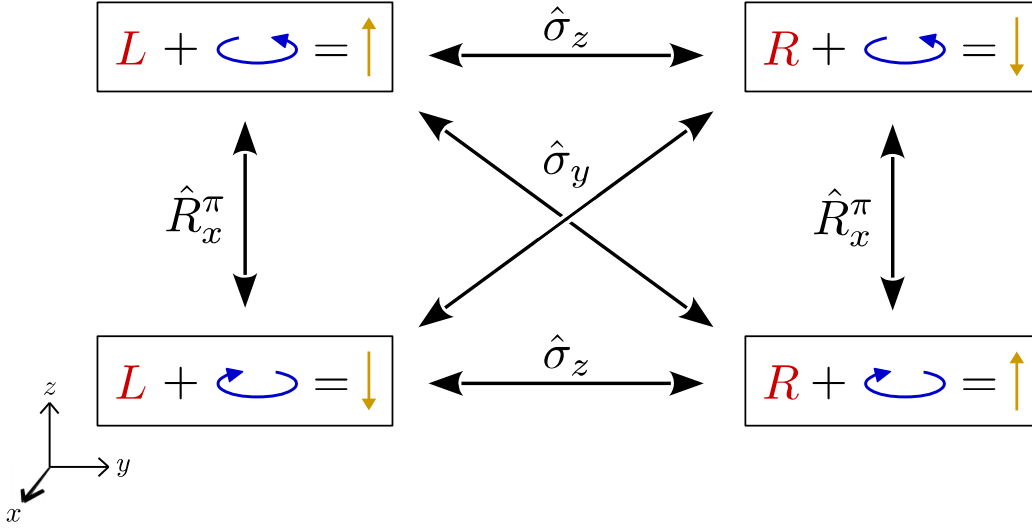


Figure 2. Symmetry properties of an isotropic ensemble of chiral molecules interacting with circularly polarized light in the electric-dipole approximation. The box represents the “enantiomer+field” system. Inside the box: red letters L and R specify the enantiomer, the curved blue arrow specifies the direction of rotation of a field circularly polarized in the xy plane, and the vertical golden arrow stands for a polar vector observable $\vec{v} = v_z \hat{z}$ displaying asymmetry with respect to the polarization xy plane. A reflection $\hat{\sigma}_z$ with respect to the xy plane, leaves the field invariant, but swaps the enantiomer and flips \vec{v} . A rotation \hat{R}_a^π by π radians around any axis \vec{a} contained in the xy plane leaves the enantiomer invariant because the ensemble is isotropic, but swaps the polarization and flips \vec{v} . Note that a rotation \hat{R}_x^π (\hat{R}_y^π) followed by a reflection $\hat{\sigma}_z$ is equivalent to a reflection $\hat{\sigma}_y$ ($\hat{\sigma}_x$) and leaves \vec{v} invariant but swaps both the enantiomer and the polarization.

Figure 2 shows that for an achiral ensemble, i.e. an ensemble of achiral molecules or a racemic mixture of chiral molecules, the system “ensemble+field” is symmetric with respect to reflection $\hat{\sigma}_z$ in the xy plane. Therefore, the vector \vec{v} must vanish, yielding a photoelectron angular distribution symmetric with respect to the plane of

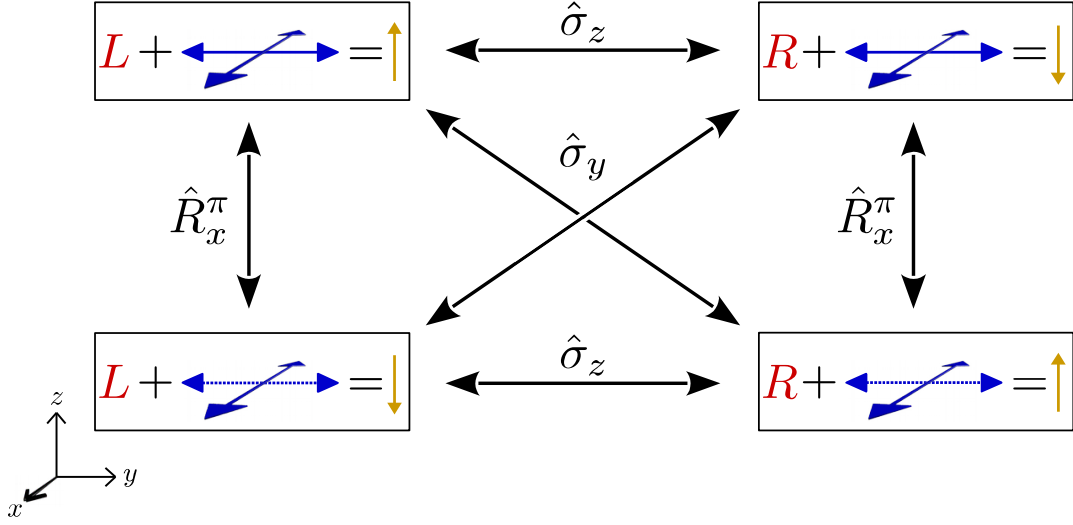


Figure 3. Same as Fig. 2 but for two perpendicular linearly polarized fields along \hat{x} (double headed arrow in perspective) and \hat{y} (horizontal double headed arrow) of arbitrary frequencies and intensities. In general $v_x \neq 0$ and $v_y \neq 0$ but only $v_z \hat{z}$ is shown (vertical arrow). A rotation \hat{R}_x^π (\hat{R}_y^π) leaves the enantiomer invariant but changes the phase of the field along \hat{y} (\hat{x}) by π . $\hat{\sigma}_x$, $\hat{\sigma}_y$, $\hat{\sigma}_z$ describe transformations of the “enantiomer+field” system upon reflections with respect to the different axes of the lab frame.

polarization, otherwise two identical experiments would yield different results. However, for a non-racemic mixture of chiral molecules, there is no symmetry enforcing $\vec{v} = 0$. Therefore, nothing prohibits the emergence of observables which display asymmetry with respect to the plane of polarization, and the associated dichroism and enantio-sensitivity. The question is what these observables are, how strong can the signal be, and what determines its limits. We address these problems in the next section.

We also stress that the cylindrical symmetry is not essential for our reasoning. The argument can be extended to other geometries including linear fields or aligned

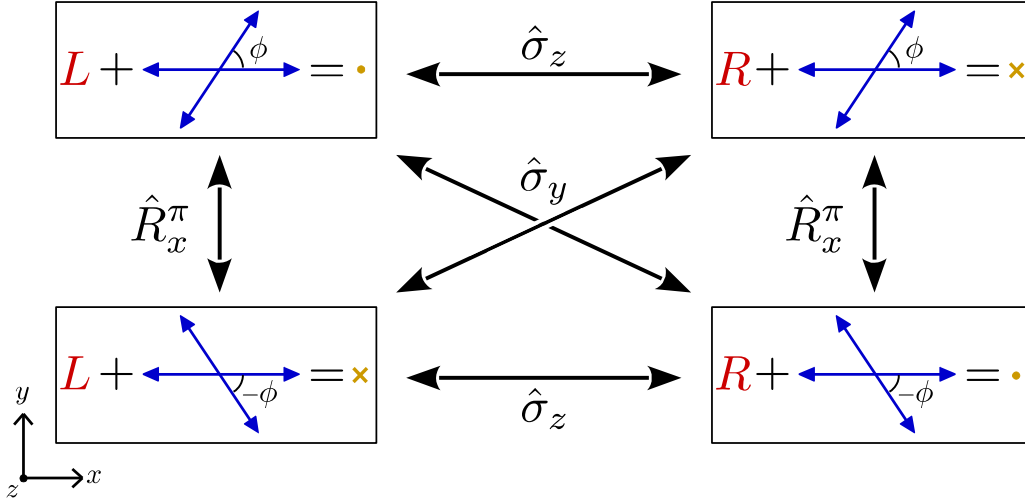


Figure 4. Same as Fig. 3 but for an arbitrary angle between the two linearly polarized fields. Note that vectors pointing out of the page are indicated by a dot (\hat{z} and \vec{v} in the upper left and lower right configurations) and vectors pointing inside the page by an \times (\vec{v} in the upper right and lower left configurations).

molecules, provided one takes into account that v_x and v_y are not necessarily zero. Figure 3 shows a generalization of the case we have just considered. Now the x and y components of the field have different frequencies, intensities, and an arbitrary phase shift with respect to each other. This field configuration is relevant, for example, for the EMWS experiments carried out in Ref. [19]. The original experiment in Ref. [16] can also be analyzed similarly by replacing one of the two-headed arrows in each “enantiomer+field” configuration in Fig. 3 by a single-headed arrow to account for the static field. The details of the analysis are discussed further in Sec. IV C, but the conclusion remains the same: the emergence of a non-vanishing polar vector characterizing the chiral response of the “enantiomer+field” system. Finally, the emergence of this vector for arbitrary orientations of linear fields is illustrated in Fig. 4.

We can now support the introductory discussion of Sec. II with several remarks concluding the symmetry analysis above:

First, from Figs. 2-4 it is clear that \vec{v} reflects the properties of the “enantiomer+field” system, and not those of the enantiomer or field separately.

Second, while it is well known that molecular chiral observables are characterized by pseudoscalars (scalar quantities that change sign upon the parity transformation), so far we have been discussing enantio-sensitive properties of a polar vector. The appearance of a polar vector \vec{v} is not accidental: its projections on the axes of the lab frame combine the information about the handedness of the chiral molecule and the handedness of the chiral setup.

Third, the observation of enantio-sensitivity and dichroism in Figs. 2-4 implicitly assumes a fixed z direction against which we can compare the rotation direction of the light and the direction of the vector \vec{v} . Otherwise, there would be no way to, for example, distinguish right- and left-circularly-polarized light from each other, since we could rotate the z axis by π to change right- into left-circularly polarized light. Although a fixed z direction is usually taken for granted, it remains physically meaningless until it is somehow related to the elements taking part in the experiment. In the methods we analyze here, such a z direction is fixed by the detector (vertical arrow in Fig. 1), which is of course assumed to remain unchanged when either the enantiomer or the light polarization is changed.

Therefore, the advent of electric-dipole-based techniques marks a shift of paradigm in chiral discrimination from using chiral reagents to using chiral observers, i.e. an experimental setup with well-defined handedness, even if the latter is not explicitly stated or recognized.

In the next section we will show that in all cases the polar vector \vec{v} is given by the product of (i) a molecular pseudoscalar and (ii) a field pseudovector specified by the

configuration of the electric fields. We will directly specify these two key quantities, forming the vectorial observables, for each of the electric-dipole-based techniques.

IV. UNIFIED DESCRIPTION OF CHIRAL ELECTRIC-DIPOLE RESPONSE

The chiral electric-dipole response manifests itself in vectorial observables, which have the following general form:

$$\vec{v} = \chi_m \vec{Z}_l, \quad (1)$$

where χ_m is a molecular pseudoscalar defining the handedness of the molecule and \vec{Z}_l is a light field pseudovector. Measuring \vec{v} means projecting it on the *external* vector \vec{u}_d defined by the detector (vertical arrow in Fig. 1),

$$\vec{v} \cdot \vec{u}_d = \chi_m \left(\vec{Z}_l \cdot \vec{u}_d \right). \quad (2)$$

The projection of \vec{Z}_l on \vec{u}_d defines the handedness of the chiral setup, therefore, the result of the measurement is given by the product of the molecular handedness and the setup's handedness. In this section we will derive χ_m and \vec{Z}_l for four different electric-dipole based techniques of chiral discrimination. These techniques include PECD [10–13], EMWS [16, 19, 20], PXCD [18], and PXECD [18].

A. Photoelectron circular dichroism

We begin with what is perhaps the most prominent electric-dipole-based technique, PECD. This technique was first proposed in 1976 [10] and then rediscovered in 1982 [11]. The first quantitative calculations of the effect [12] yielded staggering results: the expected effect was at the level of some few percent to maybe even some ten percent of the total photoionization signal. The first experiment appeared just a

year later [13]. The technique was dramatically advanced in Refs. [26–30] from a theoretical concept to an extra-sensitive experimental technique. With the advances in table-top laser-based implementations [31, 32] including multi-photon [21–23] and strong-field regimes [24], PECD has proven very interesting from both fundamental and applied perspectives. In PECD, the photoionization of an isotropic and non-racemic ensemble of chiral molecules by circularly polarized light leads to an asymmetry in the photoelectron angular distribution (PAD) with respect to the polarization plane, the so-called forward-backward asymmetry (FBA). This asymmetry is usually described by decomposing the angle-resolved photoionization probability $W(\vec{k}^L)$ in Legendre polynomials,

$$W(\vec{k}^L) = \sum_{l=0}^2 b_l(k) P_l(\cos \theta_k^L), \quad (3)$$

where it corresponds to a non-zero b_1 coefficient. In Eq. (3), $W(\vec{k}^L)$ is the probability of obtaining a photoelectron with momentum \vec{k}^L , L indicates that the vector is in the lab frame, θ_k^L is the polar angle of \vec{k}^L , $k \equiv |\vec{k}^L|$, P_l is the Legendre polynomial of degree l , and we assume that the polarization plane coincides with the $x^L y^L$ plane. The b_1 coefficient is directly related to the net photoelectron current induced by ionization

$$\vec{j}^L(k) = \int d\Omega_k^L \vec{j}^L(\vec{k}^L), \quad (4)$$

where $\vec{j}^L(\vec{k}^L) = W(\vec{k}^L)\vec{k}^L$ is the photoelectron current in the direction specified by the photoelectron direction \vec{k}^L in the lab frame, and $\int d\Omega_k^L \equiv \int_0^\pi d\theta_k^L \int_0^{2\pi} d\varphi_k^L \sin \theta_k^L$ is the integral over all photoelectron directions. From the orthogonality of the Legendre

polynomials we obtain

$$\begin{aligned}
\vec{j}^L(k) &= \int d\Omega_k^L \vec{j}^L(\vec{k}^L), \\
&= \sum_{l=0}^2 b_l(k) \int d\Omega_k^L P_l(\cos \theta_k^L) \vec{k}^L, \\
&= k \sum_{l=0}^2 b_l(k) \int d\Omega_k^L P_l(\cos \theta_k^L) P_1(\cos \theta_k^L) \hat{z}^L, \\
&= \frac{4\pi}{3} k b_1(k) \hat{z}^L,
\end{aligned} \tag{5}$$

The current in Eqs. (4) and (5) is the vectorial observable of our interest. The task is to find it or, equivalently, $b_1(k)$. The corresponding calculations of the photoelectron angular distributions traditionally rely on the formalism of angular momentum algebra, both for one-photon and few-photon PECD [10–12, 33]. We have found that it is very instructive to depart from this traditional formalism, which uses language specific for photoionization. Instead, we use an alternative, vectorial formulation, pioneered in works of Manakov [34] and applied to aligned chiral systems [35]. The vectorial formalism was also used to describe two-photon absorption CD [36]. Conveniently, it provides a common language for all electric-dipole-based techniques, irrespective of their “field of origin” or observable, be it photoionization or microwave physics.

We define the incident circularly polarized field in the lab reference frame as

$$\vec{E}(t) = \mathcal{E}(t) \hat{e}_\sigma^L + \text{c.c.} \tag{6}$$

where $\hat{e}_\sigma^L = (\hat{x}^L + i\sigma\hat{y}^L)/\sqrt{2}$ is the light polarization vector, $\sigma = \pm 1$ defines the rotation direction of the field, and $\mathcal{E}(t)$ is the time-dependent amplitude. The photoelectron current density for a given photoelectron momentum \vec{k}^M in the molecular

frame is (up to the negative electron charge)

$$\vec{j}_{\vec{k}^M}^M = |a_{\vec{k}^M}|^2 \vec{k}^M. \quad (7)$$

Here $\vec{a}_{\vec{k}^M}$ is the ionization amplitude of the transition to the continuum state $|\vec{k}^M\rangle$ from the ground state $|0\rangle$ in the circularly polarized field Eq. (6). Its standard first-order perturbation theory expression is

$$a_{\vec{k}^M} = i\tilde{\mathcal{E}} \left\langle \vec{k}^M \left| \vec{d}^L \cdot \hat{e}_\sigma^L \right| 0 \right\rangle = \frac{i\tilde{\mathcal{E}}}{\sqrt{2}} \left(\vec{D}^L \cdot \hat{x}^L + \sigma i \vec{D}^L \cdot \hat{y}^L \right), \quad (8)$$

where $\tilde{\mathcal{E}}$ is the Fourier transform of \mathcal{E} at the transition frequency, \vec{d} is the dipole operator, and \vec{D}^L is the corresponding transition dipole matrix element in the lab frame.

Our next step is to identify the molecule-specific enantio-sensitive structure in Eqs. (7) and (8). That is, we will be looking for molecule-specific pseudoscalars; quantities that change sign upon parity inversion. Pseudoscalars may arise as a product of a vector and pseudovector. An example of such pseudoscalar is the helicity η of circularly polarized light which is non-zero only beyond the electric-dipole approximation (see Appendix VII A). Molecular pseudoscalars also arise from triple products formed by three molecular polar vectors. We shall now look for such quantities.

Let us look at the cross term arising in $|a_{\vec{k}^M}|^2$,

$$i\sigma \left[(\vec{D}^{L*} \cdot \hat{x}^L)(\vec{D}^L \cdot \hat{y}^L) - (\vec{D}^L \cdot \hat{x}^L)(\vec{D}^{L*} \cdot \hat{y}^L) \right]. \quad (9)$$

We now use the vector identity $(\vec{a} \cdot \vec{c})(\vec{b} \cdot \vec{d}) - (\vec{a} \cdot \vec{d})(\vec{b} \cdot \vec{c}) = (\vec{a} \times \vec{b}) \cdot (\vec{c} \times \vec{d})$ and the fact that $\hat{x}^L \times \hat{y}^L = \hat{z}^L$ to write the interference term as a triple product,

$$|a_{\vec{k}^M}|^2 = \frac{|\tilde{\mathcal{E}}|^2}{2} \left\{ \left| \vec{D}^L \cdot \hat{x}^L \right|^2 + \left| \vec{D}^L \cdot \hat{y}^L \right|^2 + i\sigma \left(\vec{D}^{L*} \times \vec{D}^L \right) \cdot \hat{z}^L \right\}. \quad (10)$$

Note that $i(\vec{D}^* \times \vec{D}) = 2\Im\{\vec{D}\} \times \Re\{\vec{D}\}$ is a real vector, where $\Re\{\vec{D}\}$ and $\Im\{\vec{D}\}$ are the real and imaginary parts of \vec{D} .

The last term in Eq. (10) is a triple product, but it is not the one we were looking for. Indeed, instead of a polar vector, $\sigma\hat{z}^L$ is a pseudovector that characterizes the rotation direction of the field, i.e. the photon's spin (see Appendix VII A), and moreover, the triple product includes two vectors characterizing the molecule and one vector characterizing the “observer” (or the lab frame), as opposed to three vectors characterizing the molecule in the molecular frame.

To relate the above expression to the transition dipoles in the molecular, rather than the lab frame, one can use the rotation matrix $S(\varrho)$. It transforms the vectors from the molecular to the lab frame via a rotation through the Euler angles $\varrho \equiv (\alpha\beta\gamma)$: $\vec{D}^L = S\vec{D}^M \equiv S\langle\vec{k}^M|\vec{d}^M|0\rangle$.

Using Eq. (10), we can also write the current in the lab frame, corresponding to the photoelectron momentum \vec{k}^M in the molecular frame

$$\vec{j}_{\vec{k}^M}^L = S\vec{j}_{\vec{k}^M}^M = \frac{|\tilde{\mathcal{E}}|^2}{2} \left[\left| S\vec{D}^M \cdot \hat{x}^L \right|^2 + \left| S\vec{D}^M \cdot \hat{y}^L \right|^2 + \sigma i S \left(\vec{D}^{M*} \times \vec{D}^M \right) \cdot \hat{z}^L \right] S\vec{k}^M. \quad (11)$$

Note that $\vec{D}^{L*} \times \vec{D}^L = S(\vec{D}^{M*} \times \vec{D}^M)$. This current is not a usual observable. Measuring it would require a coincidence-type setup, where one would detect the lab-frame electron momentum together with the orientation of the molecular frame in the lab frame. We are interested in the standard observable – the net photoelectron current in the lab frame. Therefore, we need to integrate over all directions of the photoelectron momentum and over all molecular orientations:

$$\vec{j}^L(k) = \int d\varrho \int d\Omega_k^M \vec{j}_{\vec{k}^M}^L, \quad (12)$$

where $\int d\Omega_k^M \equiv \int_0^\pi d\theta_k^M \int_0^{2\pi} d\varphi_k^M \sin \theta_k^M$.

Within the standard approach, one performs the integration over all molecular orientations keeping the photoelectron momentum \vec{k} fixed in the lab frame. This yields the standard lab-frame photoelectron angular distributions, from which the b_1 coefficient, which is proportional to the net photoelectron current [see Eq. 5], is extracted. Here, since we are not interested in the full angular distribution of photoelectrons, we can keep the photoelectron momentum \vec{k} fixed in the molecular frame. This simplifies the orientation averaging procedure considerably because in this case the transition matrix element vector $\vec{D}^M(\vec{k}^M)$ does not have an argument that depends on the molecular orientation ϱ , and can therefore be trivially rotated as $S(\varrho)\vec{D}^M(\vec{k}^M)$. In the other case, when \vec{k} is fixed in the lab frame, the corresponding rotation reads as $S(\varrho)\vec{D}^M(S(\varrho)^{-1}\vec{k}^L)$ and the orientation averaging step requires knowing how \vec{D} changes as a function of \vec{k} , which is usually tackled with a partial wave expansion of the continuum wave function. We do not have such complication here and we can simply use the vector identity Eq. (51) derived in Appendix VII B to obtain

$$\vec{j}^L(k) = \left\{ \frac{1}{6} \int d\Omega_k^M \left[i \left(\vec{D}^{M*} \times \vec{D}^M \right) \cdot \vec{k}^M \right] \right\} \left\{ \sigma |\tilde{\mathcal{E}}|^2 \hat{z}^L \right\}. \quad (13)$$

The equivalence between expression (13) and the original expression derived by Ritchie in [10] is demonstrated in Appendix VII E.

Expression (13) is physically transparent. In particular, it shows that the strength of the chiral signal depends on the mutual orientation of the three vectors forming the triple product of vectors defined in the molecular frame.

Let us analyze expression (13):

First, we see that only the interference term in the current [see Eq. (11)] yields a non-vanishing contribution to the net current after orientation averaging. This stresses the importance of the coherence between the two contributions to the ionization amplitude, triggered by the two components of the ionizing field.

Second, we see that the orientation averaging has modified the expression for the vector triple product: it no longer involves any lab-frame quantities, such as $\sigma\hat{z}^L$. Its place is now taken by the molecular frame photoelectron momentum \vec{k}^M , and the molecular term is now a rotationally invariant quantity.

Third, Eq. (13) shows that the net photoelectron current (per molecule) in the lab frame can be factored into a pseudovector field term expressed in the lab frame and a pseudoscalar molecular term expressed in the molecular frame. The pseudovector field term contains the intensity of the field at the transition frequency, and the rotation direction of the circularly polarized field $\sigma\hat{z}^L$. The molecular term is an integral over all states on the photoelectron energy shell $k^2/2$, where, after taking into account all molecular orientations, each state contributes by an amount proportional to the scalar triple product between $\vec{D}^M(\vec{k}^M)$, $\vec{D}^{M*}(\vec{k}^M)$, and \vec{k}^M , or equivalently between $\Re\{\vec{D}^M(\vec{k}^M)\}$, $\Im\{\vec{D}^M(\vec{k}^M)\}$, and \vec{k}^M .

From the field term we can see that $\vec{j}^L(k)$ is directed along \hat{z}^L and takes opposite values for opposite circular polarizations and a given enantiomer. On the other hand, from the relationship between the photoionization dipoles of opposite enantiomers derived in Appendix VII D, $\vec{D}_{\text{left}}^M(\vec{k}^M) = -\vec{D}_{\text{right}}^M(-\vec{k}^M)$, it is simple to see that the molecular term is a pseudoscalar, i.e. it changes sign under a parity inversion, and therefore $\vec{j}^L(k)$ takes opposite values for the opposite enantiomers and a given circular polarization [see Eqs. (82) and (83) in Appendix VII D]. All these conclusions are in agreement with the symmetry analysis described in Sec. III, with $\vec{j}^L(k)$ playing the role of the generic dichroic and enantio-sensitive vector \vec{v} .

The triple product in the molecular term vanishes if the vectors are coplanar, which is for example the case for the plane wave continuum, where one can use the velocity gauge to show that \vec{D}^M is parallel to \vec{k}^M . This conclusion corresponds to the well known fact that $|\vec{j}^L(k)|/k \propto |b_1|$ has an overall tendency to decrease as the photo-electron energy increases and the continuum resembles more and more a plane wave. One can also show that $\vec{j}^L(k)$ vanishes in case of a spherically symmetric continuum in agreement with earlier studies [11]. The same conclusion holds for the strong-field PECD [25].

Our derivation and the result provide us with an important insight. The chiral signal stems from the interference between the two non-collinear dipole transitions. If we consider a single final state, such interference leading to a vector product of two transition dipoles would only be possible for a scattering state where the complex transition dipole allows for two non-collinear components: one of them is given by the real part of the transition dipole and the other by its imaginary part.

The generalization of Eq. (13) to arbitrary polarizations of the field is straightforward. We just need to separate the Fourier transform of the field into its real and imaginary parts, and keep in mind that for any complex vector $\vec{u} = \vec{u}_r + i\vec{u}_i$ we have that $\vec{u}^* \times \vec{u} = -2i\vec{u}_i \times \vec{u}_r$. Then we obtain

$$\vec{j}^L(k) = \left\{ \frac{1}{6} \int d\Omega_k^M \left[\left(\vec{D}^{M*} \times \vec{D}^M \right) \cdot \vec{k}^M \right] \right\} \left\{ \tilde{\mathcal{E}}^{L*} \times \tilde{\mathcal{E}}^L \right\}, \quad (14)$$

which reduces to Eq. (13) for the case of circularly polarized light. Eq. (14) shows that for an arbitrary field configuration the chiral response in PECD is not necessarily along the light propagation direction.

B. Photo-excitation circular dichroism in electronic or vibronic states

Let us now consider chiral response in bound excited states. In this case, and for a single excited state, the excitation dipole is real. Therefore, $\vec{D}^M(\vec{k}^M)$ and $\vec{D}^{M*}(\vec{k}^M)$ are parallel, yielding zero enantio-sensitive dipole signal.

On the other hand, if we were to coherently excite two states with non collinear transition dipoles, we would have a non-zero cross product. Then we could obtain a dichroic and enantio-sensitive signal as long as we find a vectorial signal that involves the interference between the two excitations. Unlike in the previous case where this vectorial signal was provided by the photoelectron current, in this case, it is provided by the dynamics of the induced polarization.

The goal of our analysis is to uncover the intimate connection between the PXCD effect discovered in [18] for electronic and vibronic states and the EMWS discovered in [16] for the rotational states. The physics in these two cases is quite different, as the former involves internal and the latter external degrees of freedom, leading to subtle but important details in the mathematical treatment.

Consider the case of two electronic or vibronic states, which can be coherently excited by an ultrashort pulse from the ground state. As before, we will consider a randomly oriented ensemble. After interaction with a field of arbitrary frequency, polarization, and intensity, the first-order amplitudes of the excited states are given by

$$a_j(t) = i \left[\vec{d}_{j,0}^L \cdot \tilde{\mathcal{E}}^L(\omega_{j0}) \right] e^{-i\omega_j t}, \quad j = 1, 2. \quad (15)$$

where $\vec{d}_{j,0}^L$ is now the real-valued transition dipole between the ground and j -th excited state and $\tilde{\mathcal{E}}^L$ is the Fourier transform of the field at the corresponding transition frequency. For an ultrashort pulse with the bandwidth covering both excited states, the expectation value of the dipole will contain an interference term of the form

$$\begin{aligned}
\langle \vec{d}^L \rangle_\chi &\equiv a_1^* a_2 \vec{d}_{1,2}^L + \text{c.c.} \\
&= \left[\vec{d}_{0,1}^L \cdot \tilde{\mathcal{E}}^{L*}(\omega_{1,0}) \right] \left[\vec{d}_{2,0}^L \cdot \tilde{\mathcal{E}}^L(\omega_{2,0}) \right] \vec{d}_{1,2}^L e^{-i\omega_{2,1}t} + \text{c.c.}
\end{aligned} \tag{16}$$

which we have denoted by $\langle \vec{d}^L \rangle_\chi$ to indicate that it is the chiral part of the induced polarization.

In contrast to Eq. (10) and PECD, the fact that the Fourier transform of the field is evaluated at two different transition frequencies in the above expression does not allow us to easily use the vector identity $(\vec{a} \cdot \vec{c})(\vec{b} \cdot \vec{d}) - (\vec{a} \cdot \vec{d})(\vec{b} \cdot \vec{c}) = (\vec{a} \times \vec{b}) \cdot (\vec{c} \times \vec{d})$ and directly identify a triple product. The emergence of the triple-product as an enantio-sensitive measure is somewhat subtle: it only appears after averaging over *all* molecular orientations, for a randomly oriented molecular ensemble. With the help of Eq. (52) derived in Appendix VII B, one finds that

$$\int d\varrho \langle \vec{d}^L \rangle_\chi = \frac{1}{6} \left[\left(\vec{d}_{0,1}^M \times \vec{d}_{2,0}^M \right) \cdot \vec{d}_{1,2}^M \right] \left[\tilde{\mathcal{E}}^{L*}(\omega_{1,0}) \times \tilde{\mathcal{E}}^L(\omega_{2,0}) \right] e^{-i\omega_{2,1}t} + \text{c.c.} \tag{17}$$

The essential features of this expression are similar to those of PECD. The expression again factorizes into a molecular part, a pseudoscalar given by the triple product of molecule-specific transition dipoles, and a field part, a pseudovector given by the vector product of the incident fields. The induced dipole oscillates at the frequency $\omega_{2,1}$ in the direction determined by the cross product between the Fourier transforms of the exciting fields, at the corresponding transition frequencies. The triple product of the transition dipoles is taken in the molecular frame and forms the pseudoscalar that changes sign for opposite enantiomers (see Appendix VII D). This means that the phase of the oscillations will be determined by the product of the signs resulting from the molecular and field terms. For a fixed polarization and opposite enantiomers,

or for a fixed enantiomer and opposite polarizations (see Figs. 2-4), the phase will change by π . That is, the enantio-sensitive and dichroic character of the vectorial observable, in this case the polarization, is encoded in the phase of its oscillations.

In the particular case of a circularly polarized field [see Eq.(6)], we have $\tilde{\mathcal{E}}^L(\omega) = \tilde{\mathcal{E}}(\omega) (\hat{x}^L + \sigma i \hat{y}^L) / \sqrt{2}$ and therefore

$$\int d\varrho \left\langle \vec{d}^L \right\rangle_{\chi} = \frac{i\sigma}{6} \left[\left(\vec{d}_{0,1}^M \times \vec{d}_{2,0}^M \right) \cdot \vec{d}_{1,2}^M \right] \tilde{\mathcal{E}}^*(\omega_{1,0}) \tilde{\mathcal{E}}(\omega_{2,0}) \hat{z}^L e^{-i\omega_{2,1}t} + \text{c.c.}, \quad (18)$$

which is the PXCD effect discovered in [18].

Equation (17) is the generalization of the PXCD effect to the case of an arbitrary field. It shows that one can obtain the same effect by either using a single broadband elliptically polarized pulse or, for example, by using a sequence of two spectrally narrow (and phase locked) linearly polarized pulses with orthogonal polarizations. If more than two levels are coherently excited, then Eq. (18) should include the sum over all states.

Importantly, the vectorial quantity associated with the chiral response does not have to be collinear with the direction of light propagation, as it happens in the case of a circularly polarized field. It illustrates once again, that the light propagation direction, fundamental for characterizing the chirality of a photon, does not play any role in electric-dipole-based techniques. These techniques do not use the chirality of the photon, but use the polarization vectors of the light to define the lab setup.

An important feature that distinguishes the “light-observer” from the “light-reagent” is the presence of chiral sensitive absorption. Of course, PECD is associated with light absorption, but this absorption is not chiral sensitive, e.g. it is neither enantio-sensitive nor dichroic [18].

Note that the earlier results for the quadratic susceptibility in isotropic chiral media can also be presented in the vectorial form, originally derived by Giordmaine [37],

$$\vec{P}(\omega_3 = \omega_1 - \omega_2) = \chi^{(2)}[\vec{E}_1(\omega_1) \times \vec{E}_2^*(\omega_2)], \quad (19)$$

where the vectors \vec{P} , \vec{E}_1 , and \vec{E}_2 , are the Fourier components of induced polarizations and incident fields at the respective frequencies, $\chi^{(2)}$ is the molecular pseudoscalar described by the triple product of transition dipoles and a combination of resonance denominators typical for second order instantaneous response and derived in [14, 15] in the context of tree-wave mixing in isotropic chiral media within the electric-dipole approximation.

Finally, the expression for PXCD also allows one to gauge the strength of the chiral response. It maximizes when the three transition dipoles are orthogonal to each other. In this case, the coherent enantio-sensitive dipole along the lab \hat{z}^L axis, normalized to the excitation amplitudes, reaches $d_{1,2}^M/3$. Thus, for orthogonal excitation dipoles, the molecule can convert all of its (ensemble-averaged) initial excitation in the polarization plane of the circularly polarized pump into enantio-sensitive motion orthogonal to this plane, making a highly efficient helix.

C. Chiral response upon rotational excitation: enantio-sensitive microwave spectroscopy

In this section we will use our vectorial formulation to consider two enantio-sensitive schemes in the microwave regime suggested by Patterson et al. [16, 19], and described theoretically in detail by Lehman [20].

Consider first coherent excitation of rotational states and the enantio-sensitive signal

discovered by Patterson et al. in [19]. The corresponding rotational wavefunctions are the eigenstates of the asymmetric rigid rotor [38], and are themselves functions of the Euler angles. We no longer deal with *a posteriori* averaging over this degree of freedom. The transition dipoles themselves are already the integrals over the Euler angles $\varrho \equiv (\alpha\beta\gamma)$,

$$\begin{aligned} \vec{d}_{i,j}^{\text{L}} &= \langle J_i \tau_i M_i | \vec{d}^{\text{L}} | J_j \tau_j M_j \rangle \\ &= \left[\int d\varrho \psi_{J_i \tau_i M_i}^*(\varrho) S(\varrho) \psi_{J_j \tau_j M_j}(\varrho) \right] \vec{d}^{\text{M}}, \end{aligned} \quad (20)$$

where \vec{d}^{M} is the permanent dipole moment of the electronic ground state in the molecular frame, $i, j = 1, 2$. The state $|J\tau M\rangle$ is an eigenfunction of the total angular momentum operator \hat{J}^2 and its z -component \hat{J}_z with eigenvalues $J(J+1)$ and M , respectively, and τ is associated with all other quantum numbers pertinent for this state. These transition dipoles are now used for the excitation amplitudes, which are still given by the general expression Eq. (15) and the induced dipole Eq. (16). Each of the dipoles entering Eq. (16) is associated with a distribution of possible M_i, M_j, M_k . This distribution depends on the preparation of the system.

The orientation averaging over the Euler angles is now replaced by summing over the distribution of all possible initial and final M 's

$$\sum_{M_0, M_1, M_2} \left\langle \vec{d}^{\text{L}} \right\rangle_{\chi} = \sum_{M_0, M_1, M_2} \left[\vec{d}_{0,1}^{\text{L}} \cdot \tilde{\mathcal{E}}^{\text{L}*}(\omega_{1,0}) \right] \left[\vec{d}_{2,0}^{\text{L}} \cdot \tilde{\mathcal{E}}^{\text{L}}(\omega_{2,0}) \right] \vec{d}_{1,2}^{\text{L}} e^{-i\omega_{2,1}t} + \text{c.c.} \quad (21)$$

When all possible initial and final M 's are equally represented, as is the case for an isotropic sample, the averaging is performed with the help of Eq. (56) which is

derived the Appendix (VII C) and yields

$$\sum_{M_0, M_1, M_2} \langle \vec{d}^L \rangle_\chi = \sum_{M_0, M_1, M_2} \frac{1}{6} \left[\left(\vec{d}_{0,1}^M \times \vec{d}_{2,0}^M \right) \cdot \vec{d}_{1,2}^M \right] \left[\tilde{\mathcal{E}}^{L*}(\omega_{1,0}) \times \tilde{\mathcal{E}}^L(\omega_{2,0}) \right] e^{-i\omega_{2,1}t} + \text{c.c.} \quad (22)$$

The main result here is the factorization of induced polarization into the molecular-specific pseudoscalar $\sum_{M_0, M_1, M_2} \frac{1}{6} \left[\left(\vec{d}_{0,1}^M \times \vec{d}_{2,0}^M \right) \cdot \vec{d}_{1,2}^M \right]$, and the field pseudovector $\left[\tilde{\mathcal{E}}^{L*}(\omega_{1,0}) \times \tilde{\mathcal{E}}^L(\omega_{2,0}) \right]$.

Note that before the averaging we had scalar products of dipoles and fields [see Eq. (21)]. The averaging over the distribution of M -states in Eq. (21) plays the same role as averaging over a random classical rotational ensemble in Eq. (17): it leads to rearrangement of terms and to the appearance of a rotationally invariant molecular pseudoscalar. It shows the link to the PXCD effect [18] in the vibronic states.

Eq. (22) is applicable for an arbitrary field configuration. In the work by Patterson et al. [19] two linearly polarized fields, orthogonal to each other, have been used to produce a sum-frequency signal polarized along the direction perpendicular to both fields. Here we derived the complementary difference-frequency signal.

Importantly, our result shows that, if two different pulses are used, the signal in Eqs. (17) and (22) depends on the relative phase between the two pulses. Therefore, the chiral signal will only be observed in a reproducible fashion if the relative phase between the two pulses is stable from shot to shot. Clearly, this is automatically satisfied in case of one-pulse excitation with a circularly polarized field, where the relative phase between the two perpendicular components is fixed at $\pi/2$, as it happens in PXCD.

Now we shall consider an alternative scheme, invented by Patterson et al. and involving a static field [16].

Vectorial formulation for the static field case

Consider a molecule with eigenstates $|n\rangle$ in the absence of fields and initially in the state $|0\rangle$. Application of a static field \vec{E}_S^L transforms the zeroth-order eigenstates into

$$|n'\rangle = |n\rangle + \sum_{m \neq n} \frac{\vec{E}_S^L \cdot \vec{d}_{m,n}^L}{E_{m,n}} |m\rangle, \quad (23)$$

where $E_{m,n}$ is the energy difference between the m -th and n -th states, and we assumed that the states are non-degenerate, or that the perturbation does not couple degenerate states with the same energy. If the perturbation of the initial state is much smaller than that of the excited state and we apply an oscillating field resonant with the transition $|0\rangle \rightarrow |n'\rangle$, then the first order (in the oscillating field) amplitude of the state $|n'\rangle$ reads as

$$\begin{aligned} a_{n'} &= i \left[\vec{d}_{n',0}^L \cdot \tilde{\mathcal{E}}^L(\omega_{n',0}) \right] \\ &= i \left\{ \left[\vec{d}_{n,0}^L \cdot \tilde{\mathcal{E}}^L(\omega_{n',0}) \right] + \sum_{m \neq n} \frac{\vec{E}_S^L \cdot \vec{d}_{n,m}^L}{E_{m,n}} \left[\vec{d}_{m,0}^L \cdot \tilde{\mathcal{E}}^L(\omega_{n',0}) \right] \right\}. \end{aligned} \quad (24)$$

While the DC Stark field is still present, the expected value of the dipole has the form

$$\langle \vec{d}^L \rangle = \vec{d}_{0,0}^L + |a_{n'}|^2 \vec{d}_{n',n'}^L + \left(a_{n'} \vec{d}_{0,n'}^L e^{-i\omega_{n',0}t} + \text{c.c.} \right). \quad (25)$$

Upon orientation averaging, the oscillating term reads as

$$\begin{aligned}
\int d\varrho a_{n'} \bar{d}_{0,n'}^{\mathbf{L}} e^{-i\omega_{n',0}t} + \text{c.c.} &= i \int d\varrho \left[\bar{d}_{n',0}^{\mathbf{L}} \cdot \tilde{\mathcal{E}}^{\mathbf{L}}(\omega_{n',0}) \right] \bar{d}_{0,n'}^{\mathbf{L}} e^{-i\omega_{n',0}t} + \text{c.c.} \\
&= \frac{i}{3} \left[\bar{d}_{n',0}^{\mathbf{M}} \cdot \bar{d}_{0,n'}^{\mathbf{M}} \right] \tilde{\mathcal{E}}^{\mathbf{L}}(\omega_{n',0}) e^{-i\omega_{n',0}t} + \text{c.c.}, \quad (26)
\end{aligned}$$

so that the oscillations of the induced polarization follow the field. Note that the orientation averaging for the rotational states would follow accordingly as shown above, by replacing $\int d\varrho$ by a sum over all M 's and keeping the sum on the right hand side of Eq. (26).

On the other hand, if the static field is adiabatically removed so that all of the population in state $|n'\rangle$ is transferred to state $|n\rangle$ we get

$$\langle \bar{d}^{\mathbf{L}} \rangle = \bar{d}_{0,0}^{\mathbf{L}} + |a_{n'}|^2 \bar{d}_{n,n}^{\mathbf{L}} + \left(a_{n'} \bar{d}_{0,n}^{\mathbf{L}} e^{-i\omega_{n,0}t+\phi} + \text{c.c.} \right) \quad (27)$$

where ϕ depends on the details of the turn-off of the static field. The orientation-averaged oscillating term reads as

$$\begin{aligned}
&\int d\varrho a_{n'} \bar{d}_{0,n}^{\mathbf{L}} e^{-i\omega_{n,0}t+\phi} + \text{c.c.} \\
&= i \int d\varrho \left\{ \left[\bar{d}_{n,0}^{\mathbf{L}} \cdot \tilde{\mathcal{E}}^{\mathbf{L}}(\omega_{n',0}) \right] \bar{d}_{0,n}^{\mathbf{L}} \right. \\
&\quad \left. + \sum_{m \neq n} \frac{1}{E_{m,n}} \left[\bar{d}_{n,m}^{\mathbf{L}} \cdot \vec{E}_S^{\mathbf{L}} \right] \left[\bar{d}_{m,0}^{\mathbf{L}} \cdot \tilde{\mathcal{E}}^{\mathbf{L}}(\omega_{n',0}) \right] \bar{d}_{0,n}^{\mathbf{L}} \right\} e^{-i\omega_{n,0}t+\phi} + \text{c.c.} \\
&= i \left\{ \frac{1}{3} \left[\bar{d}_{n,0}^{\mathbf{M}} \cdot \bar{d}_{0,n}^{\mathbf{M}} \right] \tilde{\mathcal{E}}^{\mathbf{L}}(\omega_{n',0}) \right. \\
&\quad \left. + \frac{1}{6} \sum_{m \neq n} \frac{1}{E_{m,n}} \left[\left(\bar{d}_{n,m}^{\mathbf{M}} \times \bar{d}_{m,0}^{\mathbf{M}} \right) \cdot \bar{d}_{0,n}^{\mathbf{M}} \right] \left[\vec{E}_S^{\mathbf{L}} \times \tilde{\mathcal{E}}^{\mathbf{L}}(\omega_{n',0}) \right] \right\} e^{-i\omega_{n,0}t+\phi} + \text{c.c.}, \quad (28)
\end{aligned}$$

In this case we obtain an enantio-sensitive contribution which oscillates in the direction specified by the cross product between the direction of the static field and the polarization of the oscillating field. If, like in the original experiment [16], the static field is along \hat{x} and the oscillating field is along \hat{z} , then the polarization will exhibit oscillations along \hat{y} .

Wave mixing phenomena are usually described on the language of susceptibilities. The quadratic susceptibility $\chi^{(2)}$ is responsible for three wave mixing. However, both PXCD and EMWS can also be described as free induction decay. In fact, PXCD maximizes when the laser field is already turned off (see Fig. 2b in Ref. [18]), supporting that free induction decay after the pulse is at its main origin.

The example of a static field is interesting because it shows that the free induction decay occurring both in PXCD and in EMWS can have very different properties from the “instantaneous” response of an isotropic chiral medium described by the quadratic susceptibility $\chi^{(2)}$. For example, as shown in [15], the chiral quadratic susceptibility vanishes if one of the excitation fields is static, while the second term in Eq. (28) shows that the chiral response associated with the free induction decay is non-zero, be it EMWS or generalized PXCD.

D. Bound-bound + bound-unbound transition

In the previous section we saw how molecular chirality can be read out from the dynamics of the induced polarization. One can also imagine reading out this chirality not by looking at the induced polarization directly but by looking at the photoelectron current induced by a second absorption process as originally proposed in [18]. Here, we will consider the general case in which a pump pulse of arbitrary polarization excites the molecule to a bound superposition and a probe pulse of arbitrary

polarization ionizes it after a time delay τ . In this case the photoionization amplitude into the state $|\vec{k}^M\rangle$ reads as

$$a_{\vec{k}^M} = - \left[\vec{d}_{1,0}^L \cdot \tilde{\mathcal{E}}_1^L(\omega_{1,0}) \right] \left[\vec{D}_1^L \cdot \tilde{\mathcal{E}}_2^L(\omega_{k,1}) \right] e^{-i\omega_1\tau} \\ - \left[\vec{d}_{2,0}^L \cdot \tilde{\mathcal{E}}_1^L(\omega_{2,0}) \right] \left[\vec{D}_2^L \cdot \tilde{\mathcal{E}}_2^L(\omega_{k,2}) \right] e^{-i\omega_2\tau}, \quad (29)$$

where $\vec{d}_{i,0}$ is a bound-bound transition dipole between states $|i\rangle$ and $|0\rangle$, \vec{D}_i is a bound-continuum transition dipole between states $|\vec{k}^M\rangle$ and $|i\rangle$, $\tilde{\mathcal{E}}_i$ is the Fourier transform of the i -th pulse, and we assumed that the pulses do not overlap. Application of Eq. (53) to Eqs. (7), (12), and (29), yields the most general result and it shows that not only the cross terms, as in the generalized PXCD [see Eq. (17)], but also the diagonal terms in $|a_{\vec{k}^M}|^2$ may contribute to the net photoelectron current

$$\vec{j}^L(k) = \int d\varrho \int d\Omega_k^M |a_{\vec{k}^M}(\varrho)|^2 S(\varrho) \vec{k}^M \\ = \vec{j}_{\text{diag},1}^L(k) + \vec{j}_{\text{diag},2}^L(k) + \vec{j}_{\text{cross}}^L(k). \quad (30)$$

The contribution from the diagonal terms is of the form

$$\vec{j}_{\text{diag},i}^L(k) = \int d\varrho \int d\Omega_k^M \left(\vec{d}_{0,i}^L \cdot \tilde{\mathcal{E}}_1^{L*} \right) \left(\vec{D}_i^{L*} \cdot \tilde{\mathcal{E}}_2^{L*} \right) \left(\vec{d}_{i,0}^L \cdot \tilde{\mathcal{E}}_1^L \right) \left(\vec{D}_i^L \cdot \tilde{\mathcal{E}}_2^L \right) \vec{k}^L \\ = \frac{1}{15} \Re \left\{ \int d\Omega_k^M \left[\left(\vec{d}_{0,i}^M \times \vec{D}_i^{M*} \right) \cdot \vec{D}_i^M \right] \left(\vec{d}_{i,0}^M \cdot \vec{k}^M \right) \left[\left(\tilde{\mathcal{E}}_1^{L*} \times \tilde{\mathcal{E}}_2^{L*} \right) \cdot \tilde{\mathcal{E}}_2^L \right] \tilde{\mathcal{E}}_1^L \right. \\ + \int d\Omega_k^M \left[\left(\vec{d}_{0,i}^M \times \vec{D}_i^{M*} \right) \cdot \vec{k}^M \right] \left(\vec{d}_{i,0}^M \cdot \vec{D}_i^M \right) \left(\tilde{\mathcal{E}}_1^L \cdot \tilde{\mathcal{E}}_2^L \right) \left(\tilde{\mathcal{E}}_1^{L*} \times \tilde{\mathcal{E}}_2^{L*} \right) \\ + \int d\Omega_k^M \left[\left(\vec{d}_{0,i}^M \times \vec{D}_i^M \right) \cdot \vec{k}^M \right] \left(\vec{d}_{i,0}^M \cdot \vec{D}_i^{M*} \right) \left(\tilde{\mathcal{E}}_1^L \cdot \tilde{\mathcal{E}}_2^{L*} \right) \left(\tilde{\mathcal{E}}_1^{L*} \times \tilde{\mathcal{E}}_2^L \right) \left. \right\} \\ + \frac{1}{30} \left| \vec{d}_{i,0}^M \right|^2 \left| \tilde{\mathcal{E}}_1^L \right|^2 \int d\Omega_k^M \left[\left(\vec{D}_i^{M*} \times \vec{D}_i^M \right) \cdot \vec{k}^M \right] \left(\tilde{\mathcal{E}}_2^{L*} \times \tilde{\mathcal{E}}_2^L \right) \quad (31)$$

where we only assumed that $\vec{d}_{0,i} = \vec{d}_{i,0}$ is real, which can always be achieved for bound states in the absence of magnetic fields. The fields $\tilde{\mathcal{E}}_1$ and $\tilde{\mathcal{E}}_2$ are evaluated at the frequencies $\omega_{i,0}$ and $\omega_{k,i}$ respectively. The last term is simply the generalized PECD from the i -th state multiplied by the population in the i -th state induced by the pump and a factor of $1/5$ that comes from the orientation averaging. The terms in curly brackets represent contributions to the current beyond the usual PECD. Each term has selection rules that are evident from its vectorial structure, and will be discussed below after considering the cross terms contribution to the photoelectron current. As usual, the molecular terms are rotationally-invariant molecule-specific pseudoscalars and the field terms are pseudovectors.

The contribution from the cross terms in $|a_{\vec{k}_M}|^2$ to the net photoelectron current $\vec{j}^L(k)$ is given in general by

$$\begin{aligned} \vec{j}_{\text{cross}}^L(k) &= \int d\varrho \int d\Omega_k^M \left(\vec{d}_{0,2}^L \cdot \tilde{\mathcal{E}}_1^{L*} \right) \left(\vec{D}_2^{L*} \cdot \tilde{\mathcal{E}}_2^{L*} \right) \left(\vec{d}_{1,0}^L \cdot \tilde{\mathcal{E}}_1^L \right) \left(\vec{D}_1^L \cdot \tilde{\mathcal{E}}_2^L \right) \vec{k}^L + \text{c.c.} \\ &= \vec{j}_{\text{noncopl}}^L(k) + \vec{j}_{\text{ellip}}^L(k) + \vec{j}_{\text{lin}}^L(k), \end{aligned} \quad (32)$$

where the fields $\tilde{\mathcal{E}}_1^{L*}$, $\tilde{\mathcal{E}}_2^{L*}$, $\tilde{\mathcal{E}}_1^L$, and $\tilde{\mathcal{E}}_2^L$ are evaluated at the frequencies $\omega_{2,0}$, $\omega_{k,2}$, $\omega_{1,0}$, and $\omega_{k,1}$, respectively, and we grouped the 10 terms according to their selection rules for the fields as follows. The first group reads as

$$\begin{aligned}
\vec{j}_{\text{noncopl}}^{\text{L}}(k) = & \frac{1}{30} \left\{ \int d\Omega_k^{\text{M}} \left[\left(\vec{d}_{0,2}^{\text{M}} \times \vec{D}_2^{\text{M}*} \right) \cdot \vec{d}_{1,0}^{\text{M}} \right] \left(\vec{D}_1^{\text{M}} \cdot \vec{k}^{\text{M}} \right) \left[\left(\tilde{\mathcal{E}}_1^{\text{L}*} \times \tilde{\mathcal{E}}_2^{\text{L}*} \right) \cdot \tilde{\mathcal{E}}_1^{\text{L}} \right] \tilde{\mathcal{E}}_2^{\text{L}} \right. \\
& + \int d\Omega_k^{\text{M}} \left[\left(\vec{d}_{0,2}^{\text{M}} \times \vec{D}_2^{\text{M}*} \right) \cdot \vec{D}_1^{\text{M}} \right] \left(\vec{d}_{1,0}^{\text{M}} \cdot \vec{k}^{\text{M}} \right) \left[\left(\tilde{\mathcal{E}}_1^{\text{L}*} \times \tilde{\mathcal{E}}_2^{\text{L}*} \right) \cdot \tilde{\mathcal{E}}_2^{\text{L}} \right] \tilde{\mathcal{E}}_1^{\text{L}} \\
& + \int d\Omega_k^{\text{M}} \left[\left(\vec{d}_{0,2}^{\text{M}} \times \vec{d}_{1,0}^{\text{M}} \right) \cdot \vec{D}_1^{\text{M}} \right] \left(\vec{D}_2^{\text{M}*} \cdot \vec{k}^{\text{M}} \right) \left[\left(\tilde{\mathcal{E}}_1^{\text{L}*} \times \tilde{\mathcal{E}}_1^{\text{L}} \right) \cdot \tilde{\mathcal{E}}_2^{\text{L}} \right] \tilde{\mathcal{E}}_2^{\text{L}*} \\
& + \int d\Omega_k^{\text{M}} \left[\left(\vec{D}_2^{\text{M}*} \times \vec{d}_{1,0}^{\text{M}} \right) \cdot \vec{D}_1^{\text{M}} \right] \left(\vec{d}_{0,2}^{\text{M}} \cdot \vec{k}^{\text{M}} \right) \left[\left(\tilde{\mathcal{E}}_2^{\text{L}*} \times \tilde{\mathcal{E}}_1^{\text{L}} \right) \cdot \tilde{\mathcal{E}}_2^{\text{L}} \right] \tilde{\mathcal{E}}_1^{\text{L}*} \right\} e^{i\omega_{21}\tau} \\
& + \text{c.c.}, \tag{33}
\end{aligned}$$

and contains all the terms involving scalar triple products of the field vectors, which means that each of its terms vanishes if the fields involved in its triple product are coplanar. It means that exciting $\vec{j}_{\text{noncopl}}^{\text{L}}(k)$ requires non-collinear geometry of pump and probe pulses. For fields with the same polarization at the two transition frequencies, that is, $\tilde{\mathcal{E}}_1^{\text{L}}(\omega_{1,0}) \parallel \tilde{\mathcal{E}}_1^{\text{L}}(\omega_{2,0})$ and $\tilde{\mathcal{E}}_2^{\text{L}}(\omega_{k,1}) \parallel \tilde{\mathcal{E}}_2^{\text{L}}(\omega_{k,2})$, $\vec{j}_{\text{noncopl}}^{\text{L}}$ vanishes unless the polarization of the pump and the probe are non-coplanar, which means that at least one of the fields must be elliptically polarized. The other field can be either linearly or elliptically polarized, provided its polarization is non-coplanar to that of the first field.

The second group of contributions to $\vec{j}_{\text{cross}}^{\text{L}}$ is given by

$$\begin{aligned}
\vec{j}_{\text{ellip}}^{\text{L}}(k) = & \frac{1}{30} \left\{ \int d\Omega_k^{\text{M}} \left[\left(\vec{d}_{0,2}^{\text{M}} \times \vec{d}_{1,0}^{\text{M}} \right) \cdot \vec{k}^{\text{M}} \right] \left(\vec{D}_2^{\text{M}*} \cdot \vec{D}_1^{\text{M}} \right) \left(\tilde{\mathcal{E}}_2^{\text{L}*} \cdot \tilde{\mathcal{E}}_2^{\text{L}} \right) \left(\tilde{\mathcal{E}}_1^{\text{L}*} \times \tilde{\mathcal{E}}_1^{\text{L}} \right) \right. \\
& + \int d\Omega_k^{\text{M}} \left[\left(\vec{D}_2^{\text{M}*} \times \vec{D}_1^{\text{M}} \right) \cdot \vec{k}^{\text{M}} \right] \left(\vec{d}_{0,2}^{\text{M}} \cdot \vec{d}_{1,0}^{\text{M}} \right) \left(\tilde{\mathcal{E}}_1^{\text{L}*} \cdot \tilde{\mathcal{E}}_1^{\text{L}} \right) \left(\tilde{\mathcal{E}}_2^{\text{L}*} \times \tilde{\mathcal{E}}_2^{\text{L}} \right) \right\} e^{i\omega_{21}\tau} \\
& + \text{c.c.} \tag{34}
\end{aligned}$$

and contains the two terms involving a cross product between a single field at the two transition frequencies. For fields satisfying $\tilde{\mathcal{E}}_1^L(\omega_{1,0}) \parallel \tilde{\mathcal{E}}_1^L(\omega_{2,0})$ and $\tilde{\mathcal{E}}_2^L(\omega_{k,1}) \parallel \tilde{\mathcal{E}}_2^L(\omega_{k,2})$, each term vanishes unless the field in the cross product is elliptically polarized. The field in the scalar product can have any polarization.

The third group of contributions to \vec{j}_{cross}^L reads as

$$\begin{aligned} \vec{j}_{\text{lin}}^L(k) = & \frac{1}{30} \left\{ \int d\Omega_k^M \left[\left(\vec{d}_{0,2}^M \times \vec{D}_2^{M*} \right) \cdot \vec{k}^M \right] \left(\vec{d}_{1,0}^M \cdot \vec{D}_1^M \right) \left(\tilde{\mathcal{E}}_1^L \cdot \tilde{\mathcal{E}}_2^L \right) \left(\tilde{\mathcal{E}}_1^{L*} \times \tilde{\mathcal{E}}_2^{L*} \right) \right. \\ & + \int d\Omega_k^M \left[\left(\vec{d}_{0,2}^M \times \vec{D}_1^M \right) \cdot \vec{k}^M \right] \left(\vec{D}_2^{M*} \cdot \vec{d}_{1,0}^M \right) \left(\tilde{\mathcal{E}}_2^{L*} \cdot \tilde{\mathcal{E}}_1^L \right) \left(\tilde{\mathcal{E}}_1^{L*} \times \tilde{\mathcal{E}}_2^L \right) \\ & + \int d\Omega_k^M \left[\left(\vec{D}_2^{M*} \times \vec{d}_{1,0}^M \right) \cdot \vec{k}^M \right] \left(\vec{d}_{0,2}^M \cdot \vec{D}_1^M \right) \left(\tilde{\mathcal{E}}_1^{L*} \cdot \tilde{\mathcal{E}}_2^L \right) \left(\tilde{\mathcal{E}}_2^{L*} \times \tilde{\mathcal{E}}_1^L \right) \\ & \left. + \int d\Omega_k^M \left[\left(\vec{d}_{1,0}^M \times \vec{D}_1^M \right) \cdot \vec{k}^M \right] \left(\vec{d}_{0,2}^M \cdot \vec{D}_2^{M*} \right) \left(\tilde{\mathcal{E}}_1^{L*} \cdot \tilde{\mathcal{E}}_2^{L*} \right) \left(\tilde{\mathcal{E}}_1^L \times \tilde{\mathcal{E}}_2^L \right) \right\} e^{i\omega_{21}\tau} \\ & + \text{c.c.} \end{aligned} \quad (35)$$

and contains the remaining terms. Unlike $\vec{j}_{\text{noncpl}}^L$ and \vec{j}_{ellip}^L , which vanish in the absence of elliptical fields when $\tilde{\mathcal{E}}_1^L(\omega_{1,0}) \parallel \tilde{\mathcal{E}}_1^L(\omega_{2,0})$ and $\tilde{\mathcal{E}}_2^L(\omega_{k,1}) \parallel \tilde{\mathcal{E}}_2^L(\omega_{k,2})$, \vec{j}_{lin}^L can be non-zero even for purely linear fields provided pump and probe are neither parallel nor orthogonal to each other. Clearly, the selection rules described for $\vec{j}_{\text{noncpl}}^L$, \vec{j}_{lin}^L , and \vec{j}_{ellip}^L are also valid for the first, the second and third, and the last term of \vec{j}_{diag}^L , respectively.

As a whole, the 10 terms in Eq. (32) correspond to the 10 ways in which the five molecular vectors $\vec{d}_{0,1}^M$, $\vec{d}_{2,0}^M$, \vec{D}_1^M , \vec{D}_2^M , and \vec{k}^M can form a rotation-invariant molecular quantity. Each molecular term is coupled to a field term that corresponds to 1 of the 10 ways that a vector can be formed via scalar and vector products between 4 vectors. Unlike the diagonal terms, the cross terms contribution oscillates with

the pump-probe time delay at a frequency corresponding to the energy difference between the two bound states excited by the pump.

If we consider the PXECD setup originally described in [18], where the pump field is circularly polarized like in Eq. (6) and the pump is linearly polarized along \hat{x}^L , then application of the above discussed selection rules and some vector algebra (see Appendix VII F) yields

$$\vec{j}^L(k) = \frac{i\sigma}{60} \tilde{\mathcal{E}}_1^* \tilde{\mathcal{E}}_2^* \tilde{\mathcal{E}}_1 \tilde{\mathcal{E}}_2 \left[\left(\vec{d}_{0,1}^M \times \vec{d}_{2,0}^M \right) \cdot \int d\Omega_k^M \vec{D}_{12}^M(\vec{k}^M) \right] \hat{z}^L e^{i\omega_{21}\tau} + \text{c.c.}, \quad (36)$$

$$\vec{D}_{12}^M(\vec{k}^M) = -4 \left(\vec{D}_1^M \cdot \vec{D}_2^{M*} \right) \vec{k}^M + \left(\vec{D}_2^{M*} \cdot \vec{k}^M \right) \vec{D}_1^M + \left(\vec{D}_1^M \cdot \vec{k}^M \right) \vec{D}_2^{M*}, \quad (37)$$

which coincides with the result originally obtained in [18]. Eqs. (30), (31), (32), (33), (34), and (35) are the generalization of PXECD to arbitrary polarizations of the pump and probe pulses.

Interestingly, although the symmetry of a linear pump - linear probe scheme where the two fields are orthogonal to each other does not forbid the emergence of a non-zero net photoelectron current \vec{j}^L (see Fig. 3), Eqs. (30), (31), (32), (33), (34), and (35) show that it vanishes. This symmetry can be traced back to the fact that the phase shift between the pump and the probe is not recorded by the system because the probe step corresponds to the parametric process in terms of non-linear optics diagrams (see Fig. 1 in Ref. [18]), where the initial and final states are the same: it is a superposition of the states prepared by the pump. It highlights the fact that all the effects considered in this section do not require a phase-lock between the pump and probe pulses.

V. CONCLUSIONS

We have presented a unified approach to electric-dipole-based methods of chiral discrimination. The approach is based on a vectorial formulation of the chiral response and provides a common language for understanding electric-dipole-based techniques used in different fields, such as photoionization and microwave spectroscopy. All these techniques make use of coherent excitation of several states leading to electronic, vibronic, rotational, or ionization dynamics.

The chiral response in all cases is characterized by a vectorial observable and takes place within a chiral setup. Unlike scalar observables (e.g. total cross sections), vectorial observables (e.g. induced polarization) are able to exploit the chirality of such setups and therefore provide the opportunity to probe the chirality of isotropic molecular samples without relying on the chirality of the light inducing the response. Chiral setups can result from the combination of at least two linearly polarized fields with non-collinear polarizations (and phase-delayed in the case of a single frequency) defining a non-zero pseudovector, and a detector defining a direction parallel or anti-parallel to the field pseudovector. Furthermore, the fields defining the pseudovector need not overlap in time, which allows for pump-probe schemes in the construction of the chiral setup.

We have shown that the generic structure of the vectorial observable is given by the product of the field pseudovector, defined by the configurations of the electric fields exciting or probing chiral dynamics, and a molecular pseudoscalar characterizing the molecular handedness. The projection of the vectorial observable on the *external* direction defined by the detector yields the result of the measurement: a product between the molecular pseudoscalar associated to the molecular handedness, and the chiral setup pseudoscalar defining the handedness of the chiral setup.

The molecular pseudoscalar is given by a rotationally invariant molecule-specific quantity such as a triple product involving three bound-bound transition dipoles, and/or the triple product between photoionization dipoles and the photoelectron momentum integrated over all directions. The strength of the chiral response is determined by the mutual orientation of such vectors in the molecular frame.

The affinity of different electric-dipole-based techniques should help us to identify general mechanisms of chiral response, driven exclusively by the electric component of the electromagnetic field, and their link to molecular chiral structure and dynamics.

VI. ACKNOWLEDGEMENTS

O.S. gratefully acknowledges illuminating discussions with Prof. Aephraim Steinberg, in particular, on the role of the chiral observer in detecting the chiral response in electric-dipole-based methods. We also thank Dr. Emilio Pisanty for his comments on the role of the chiral setup in PECD. The authors are grateful to Prof. Misha Ivanov for stimulating discussions and comments on the manuscript. O.S. thanks Dr. Alex G. Harvey and Dr. Zdeněk Mašín for useful discussions. We thank Dr. Laurent Nahon and Prof. Christiane Koch for their comments on the manuscript and Prof. Amar Vutha for discussions of the EMWS scenarios. A.F.O. gratefully acknowledges the MEDEA project, which has received funding from the European Union’s Horizon 2020 research and innovation programme under the Marie Skłodowska-Curie grant agreement No 641789. O.S. gratefully acknowledges the QUTIF programme of the Deutsche Forschungsgemeinschaft, project Sm 292-5/1.

VII. APPENDIX

A. Beyond the electric-dipole approximation: the magnetic dipole, the helicity of light, and absorption circular dichroism

In order to introduce the reader into some fundamental aspects of the discussion in the main part of the manuscript, we will briefly illustrate the relation between magnetic dipole, helicity of light, and absorption circular dichroism in randomly oriented chiral molecules.

The interaction between the electron in the molecule and the radiation field can be described by the interaction Hamiltonian (see e.g. [39])

$$H'(t) = -\vec{d} \cdot \vec{E}(0, t) - \vec{m} \cdot \vec{B}(0, t) + \dots \quad (38)$$

where \vec{d} and \vec{m} are the electric and magnetic dipoles,

$$\vec{E}(\vec{r}, t) = -\partial_t \vec{A}(\vec{r}, t) \quad \text{and} \quad \vec{B}(\vec{r}, t) = \vec{\nabla} \times \vec{A}(\vec{r}, t) \quad (39)$$

are the electric and magnetic fields, and $\vec{A}(\vec{r}, t)$ is the vector potential. Other terms of the same order as the magnetic-dipole interaction (e.g. the electric-quadrupole interaction) have been ignored because electric-quadrupole effects vanish in isotropic samples [39]. Consider a plane wave with wave number \vec{k} and frequency ω ,

$$\vec{A}(\vec{r}, t) = \vec{\mathcal{A}} e^{i(\vec{k} \cdot \vec{r} - \omega t)} + \text{c.c.}, \quad (40)$$

where $\vec{\mathcal{A}}$ encodes the polarization, intensity, and phase shift of the wave. For wavelengths λ much greater than the electron orbit, the term $\vec{k} \cdot \vec{r} = 2\pi r/\lambda$ is very small

and $e^{i\vec{k}\cdot\vec{r}}$ can be expanded in powers of it. The electric-dipole and magnetic-dipole interactions in Eq. (38) stem from the zeroth and first order terms, respectively, of such expansion. That is, the magnetic-dipole interaction emerges as a consequence of taking into account the spatial structure of the electromagnetic field. Furthermore, absorption circular dichroism, which is linear in the magnetic-dipole interaction, scales as $\vec{k}\cdot\vec{r}$, i.e. as the ratio of the electron orbit size to the wavelength.

Replacing Eq. (40) in Eq. (39) yields

$$\vec{E}(0, t) = \vec{\mathcal{E}}e^{-i\omega t} + \text{c.c.} \quad \text{and} \quad \vec{B}(0, t) = \vec{\mathcal{B}}e^{-i\omega t} + \text{c.c.}, \quad (41)$$

where $\vec{\mathcal{E}} = \omega\vec{\mathcal{A}}$ and $\vec{\mathcal{B}} = i\vec{k} \times \vec{\mathcal{A}}$. Therefore, the probability that the molecule in the initial state $|i\rangle$ is excited into the upper energy state $|f\rangle$ is given by

$$|\langle f | H'(t) | i \rangle|^2 \propto \left| \left(\vec{d}_{fi} \cdot \vec{\mathcal{E}} + \vec{m}_{fi} \cdot \vec{\mathcal{B}} \right) \right|^2 \quad (42)$$

and contains an interference term of the form

$$\left(\vec{d}_{fi} \cdot \vec{\mathcal{E}} \right)^* \left(\vec{m}_{fi} \cdot \vec{\mathcal{B}} \right) + \text{c.c.} \quad (43)$$

For the case of electronic and/or vibrational transitions, \vec{d}_{fi} and \vec{m}_{fi} are fixed in the molecular frame, while $\vec{\mathcal{E}}$ and $\vec{\mathcal{B}}$ are fixed in the lab frame. If the sample is isotropic we must average over all molecular orientations ϱ (see Appendix VII B), which yields

$$\int d\varrho \left[\vec{d}_{fi}^L(\varrho) \cdot \vec{\mathcal{E}}^L \right]^* \left[\vec{m}_{fi}^L(\varrho) \cdot \vec{\mathcal{B}}^L \right] = \frac{1}{3} \left[\vec{d}_{fi}^M \cdot \vec{m}_{fi}^M \right] \left[\vec{\mathcal{E}}^{L*} \cdot \vec{\mathcal{B}}^L \right], \quad (44)$$

where the superscripts L and M indicate vectors expressed in the lab and molecular frames respectively, and we explicitly indicated the dependence of the molecular

frame vectors \vec{d}_{fi} and \vec{m}_{fi} on the molecular orientation ϱ when they are expressed in the lab frame. The right hand side of Eq. (44) is a scalar that is the product of two pseudoscalars. One of them contains only molecular quantities in the molecular frame, and the other contains only field quantities in the lab frame. Furthermore, the latter is proportional to the helicity of the field, i.e. it is proportional to the projection of the light spin angular momentum on the propagation direction \vec{k} . To see this, we rewrite the field pseudoscalar in terms of the vector potential as

$$\vec{\mathcal{E}}^{\text{L}*} \cdot \vec{\mathcal{B}}^{\text{L}} = \omega \vec{\mathcal{A}}^{\text{L}*} \cdot (\text{i} \vec{k}^{\text{L}} \times \vec{\mathcal{A}}^{\text{L}}) = \omega (\text{i} \vec{\mathcal{A}}^{\text{L}} \times \vec{\mathcal{A}}^{\text{L}*}) \cdot \vec{k}^{\text{L}}. \quad (45)$$

The factor $\text{i} \vec{\mathcal{A}}^{\text{L}} \times \vec{\mathcal{A}}^{\text{L}*}$ is always real and it is proportional to the photon's spin. For example, for light circularly polarized in the xy plane $\vec{\mathcal{A}}^{\text{L}} = \mathcal{A} (\hat{x}^{\text{L}} + \text{i} \sigma \hat{y}^{\text{L}}) / \sqrt{2}$, $\sigma = \pm 1$, and $\text{i} \vec{\mathcal{A}}^{\text{L}} \times \vec{\mathcal{A}}^{\text{L}*} = |\mathcal{A}|^2 \sigma \hat{z}^{\text{L}}$, where $\sigma \hat{z}^{\text{L}}$ is the spin of the photon. If we now project on the propagation direction \hat{k}^{L} , we obtain the sign of the helicity of the circularly polarized field

$$\eta = \sigma \hat{z}^{\text{L}} \cdot \hat{k}^{\text{L}} = \pm \sigma, \quad (46)$$

where we used the fact that \vec{k}^{L} can point either in the positive (+) or negative (-) \hat{z}^{L} direction. One must be careful of not confusing σ with η . While η indicates the handedness of the helix formed by the electric (or magnetic) component of the circularly polarized field in space at a fixed time and is a time-even pseudoscalar, σ merely indicates the direction of rotation of the electric field in time at a fixed point in space, is invariant with respect to parity inversion, and is therefore a time-odd scalar.

Importantly for the discussion in the main part of the manuscript, in the electric-dipole approximation the variation of the electromagnetic field in space and along

with it the propagation direction of the light, the magnetic field, and the magnetic-dipole interaction, are absent. Therefore, the chiral effects which rely only on the electric-dipole interaction do not rely on the helicity of the light, but on its spin. In other words, they do not rely on the pseudoscalar character of the light encoded in η but instead on its time-odd character encoded in the pseudovector $\sigma\hat{z}$.

B. Classical orientation averaging

Following the formalism in Sec. 4.2 of Ref. [39] we can perform the orientation averaging using tensor notation as follows: first we define the transformation from the molecular frame to the lab frame via

$$v_i = l_{i\alpha} v_\alpha, \quad (47)$$

where we used Einstein's summation convention, latin and greek indices indicate components in the lab and molecular frame respectively, and $l_{i\alpha}$ stands for the direction cosine between the axis $i = x^L, y^L, z^L$ in the lab frame and the axis $\alpha = x^M, y^M, z^M$ in the molecular frame. The direction cosines can be written in terms of the Euler angles $\varrho \equiv (\alpha\beta\gamma)$ (see for example Sec. 2.2 in Ref. [38]). From Sec. 4.2.5 of Ref. [39] (see also [40]) we have that the isotropic orientation averages of products of direction cosines are

$$\int d\varrho l_{i\alpha} l_{j\beta} = \frac{1}{3} \delta_{ij} \delta_{\alpha\beta}, \quad (48)$$

$$\int d\varrho l_{i\alpha} l_{j\beta} l_{k\gamma} = \frac{1}{6} \epsilon_{ijk} \epsilon_{\alpha\beta\gamma}, \quad (49)$$

$$\begin{aligned}
\int d\varrho l_{i\alpha} l_{j\beta} l_{k\gamma} l_{l\delta} l_{m\epsilon} = & \frac{1}{30} \left\{ \epsilon_{ijk} \delta_{lm} \epsilon_{\alpha\beta\gamma} \delta_{\delta\epsilon} + \epsilon_{ijl} \delta_{km} \epsilon_{\alpha\beta\delta} \delta_{\gamma\epsilon} \right. \\
& + \epsilon_{ijm} \delta_{kl} \epsilon_{\alpha\beta\epsilon} \delta_{\gamma\delta} + \epsilon_{ikl} \delta_{jm} \epsilon_{\alpha\gamma\delta} \delta_{\beta\epsilon} \\
& + \epsilon_{ikm} \delta_{jl} \epsilon_{\alpha\gamma\epsilon} \delta_{\beta\delta} + \epsilon_{ilm} \delta_{jk} \epsilon_{\alpha\delta\epsilon} \delta_{\beta\gamma} \\
& + \epsilon_{jkl} \delta_{im} \epsilon_{\beta\gamma\delta} \delta_{\alpha\epsilon} + \epsilon_{jkm} \delta_{il} \epsilon_{\beta\gamma\epsilon} \delta_{\alpha\delta} \\
& \left. + \epsilon_{jlm} \delta_{ik} \epsilon_{\beta\delta\epsilon} \delta_{\alpha\gamma} + \epsilon_{klm} \delta_{ij} \epsilon_{\gamma\delta\epsilon} \delta_{\alpha\beta} \right\} \quad (50)
\end{aligned}$$

where $\int d\varrho \equiv \frac{1}{8\pi^2} \int_0^{2\pi} d\alpha \int_0^\pi d\beta \int_0^{2\pi} d\gamma \sin\beta$. Straightforward application of formulas (48), (49), and (50) yields the vector identities

$$\int d\varrho (\vec{a}^L \cdot \vec{v}^L) \vec{b}^L = \frac{1}{3} (\vec{a}^M \cdot \vec{b}^M) \vec{v}^L, \quad (51)$$

$$\int d\varrho (\vec{a}^L \cdot \vec{u}^L) (\vec{b}^L \cdot \vec{v}^L) \vec{c}^L = \frac{1}{6} [(\vec{a}^M \times \vec{b}^M) \cdot \vec{c}^M] (\vec{u}^L \times \vec{v}^L), \quad (52)$$

$$\begin{aligned}
& \int d\varrho \left(\vec{a}^L \cdot \vec{u}^L \right) \left(\vec{b}^L \cdot \vec{v}^L \right) \left(\vec{c}^L \cdot \vec{w}^L \right) \left(\vec{d}^L \cdot \vec{x}^L \right) \vec{e}^L \\
&= \frac{1}{30} \left\{ \left[\left(\vec{a}^M \times \vec{b}^M \right) \cdot \vec{c}^M \right] \left(\vec{d}^M \cdot \vec{e}^M \right) \left[\left(\vec{u}^L \times \vec{v}^L \right) \cdot \vec{w}^L \right] \vec{x}^L \right. \\
&\quad + \left[\left(\vec{a}^M \times \vec{b}^M \right) \cdot \vec{d}^M \right] \left(\vec{c}^M \cdot \vec{e}^M \right) \left[\left(\vec{u}^L \times \vec{v}^L \right) \cdot \vec{x}^L \right] \vec{w}^L \\
&\quad + \left[\left(\vec{a}^M \times \vec{b}^M \right) \cdot \vec{e}^M \right] \left(\vec{c}^M \cdot \vec{d}^M \right) \left(\vec{u}^L \times \vec{v}^L \right) \left(\vec{w}^L \cdot \vec{x}^L \right) \\
&\quad + \left[\left(\vec{a}^M \times \vec{c}^M \right) \cdot \vec{d}^M \right] \left(\vec{b}^M \cdot \vec{e}^M \right) \left[\left(\vec{u}^L \times \vec{w}^L \right) \cdot \vec{x}^L \right] \vec{v}^L \\
&\quad + \left[\left(\vec{a}^M \times \vec{c}^M \right) \cdot \vec{e}^M \right] \left(\vec{b}^M \cdot \vec{d}^M \right) \left(\vec{u}^L \times \vec{w}^L \right) \left(\vec{v}^L \cdot \vec{x}^L \right) \\
&\quad + \left[\left(\vec{a}^M \times \vec{d}^M \right) \cdot \vec{e}^M \right] \left(\vec{b}^M \cdot \vec{c}^M \right) \left(\vec{u}^L \times \vec{x}^L \right) \left(\vec{v}^L \cdot \vec{w}^L \right) \\
&\quad + \left[\left(\vec{b}^M \times \vec{c}^M \right) \cdot \vec{d}^M \right] \left(\vec{a}^M \cdot \vec{e}^M \right) \left[\left(\vec{v}^L \times \vec{w}^L \right) \cdot \vec{x}^L \right] \vec{u}^L \\
&\quad + \left[\left(\vec{b}^M \times \vec{c}^M \right) \cdot \vec{e}^M \right] \left(\vec{a}^M \cdot \vec{d}^M \right) \left(\vec{v}^L \times \vec{w}^L \right) \left(\vec{u}^L \cdot \vec{x}^L \right) \\
&\quad + \left[\left(\vec{b}^M \times \vec{d}^M \right) \cdot \vec{e}^M \right] \left(\vec{a}^M \cdot \vec{c}^M \right) \left(\vec{v}^L \times \vec{x}^L \right) \left(\vec{u}^L \cdot \vec{w}^L \right) \\
&\quad \left. + \left[\left(\vec{c}^M \times \vec{d}^M \right) \cdot \vec{e}^M \right] \left(\vec{a}^M \cdot \vec{b}^M \right) \left(\vec{w}^L \times \vec{x}^L \right) \left(\vec{u}^L \cdot \vec{v}^L \right) \right\} \quad (53)
\end{aligned}$$

for arbitrary vectors \vec{a} , \vec{b} , \vec{c} , \vec{d} , \vec{e} , \vec{u} , \vec{v} , \vec{w} , and \vec{x} , respectively.

C. Quantum orientation averaging

In this appendix we will derive the identities

$$\sum_{M_i} \vec{A}_{i,i} = 0, \quad (54)$$

$$\sum_{M_i, M_j} \left(\vec{A}_{i,j} \cdot \vec{u} \right) \vec{A}_{j,i} = \frac{1}{3} \sum_{M_i, M_j} \left(\vec{A}_{i,j} \cdot \vec{A}_{j,i} \right) \vec{u}, \quad (55)$$

$$\sum_{M_i, M_j, M_k} \left(\vec{A}_{i,j} \cdot \vec{u} \right) \left(\vec{B}_{k,i} \cdot \vec{v} \right) \vec{C}_{j,k} = \frac{1}{6} \sum_{M_i, M_j, M_k} \left[\left(\vec{A}_{i,j} \times \vec{B}_{k,i} \right) \cdot \vec{C}_{j,k} \right] (\vec{u} \times \vec{v}), \quad (56)$$

where \hat{A} , \hat{B} , and \hat{C} , are vector operators, \vec{u} and \vec{v} are vectors, and we use the shorthand notation $\vec{A}_{i,j} = \langle \alpha_i J_i M_i | \hat{A} | \alpha_j J_j M_j \rangle$. The state $|\alpha J M\rangle$ is an eigenfunction of the total angular momentum operator \hat{J}^2 and of its z component \hat{J}_z , with eigenvalues $J(J+1)$ and M respectively. The label α indicates all the other quantum numbers required to describe the state.

These equations can be used to carry out the orientation averaging procedure of the expected value of the dipole in Sec. [IV C](#).

The first identity is rather trivial, especially in view of its classical analogue. The second and third identities are the quantum analogues of Eqs. [\(51\)](#) and [\(52\)](#) respectively. The proofs below are valid both for integer and half-integer J .

Before going into the derivation we will briefly remind the reader of a few formulas that we will use throughout our derivation. The spherical components of a vector are defined by (see Eq. 4.10 in [\[41\]](#))

$$v_0 = v_z, \quad v_{\pm} = \mp \frac{1}{\sqrt{2}} (v_x \pm i v_y). \quad (57)$$

From this definition it follows that the dot product, the cross product, and the scalar triple product can be written in terms of their spherical components as follows:

$$\vec{u} \cdot \vec{v} = \sum_{q=-1}^1 (-1)^q u_{-q} v_q \quad (58)$$

$$(\vec{u} \times \vec{v})_p = (-1)^p i \sum_{q,r=-1}^1 \epsilon_{pqr} u_{-q} v_{-r} \quad (59)$$

$$(\vec{u} \times \vec{v}) \cdot \vec{w} = -i \sum_{p,q,r=-1}^1 \epsilon_{pqr} u_p v_q w_r \quad (60)$$

where ϵ_{pqr} is the Levi-Civita tensor for the set $\{-1, 0, 1\}$ such that $\epsilon_{-1,0,1} = \epsilon_{0,1,-1} = \epsilon_{1,-1,0} = 1$ and $\epsilon_{1,0,-1} = \epsilon_{-1,1,0} = \epsilon_{0,-1,1} = -1$, and every other component is equal to zero. Note also that

$$\frac{1}{\sqrt{6}} \begin{pmatrix} 1 & 1 & 1 \\ -1 & 0 & 1 \end{pmatrix} = 1, \quad (61)$$

which along with the symmetry properties of the 3-j symbol for column permutations implies that (see also Sec. 3.2 in [41])

$$\sqrt{6} \begin{pmatrix} 1 & 1 & 1 \\ p & q & r \end{pmatrix} = \epsilon_{pqr}. \quad (62)$$

Another special value of the 3-j symbol is obtained by considering the coupling to zero angular momentum $\langle JM; 00 | JM \rangle = 1$ and the relationship between the Clebsch-Gordan coefficient and the 3-j symbol, which yields

$$\begin{pmatrix} J & 0 & J \\ -M & 0 & M \end{pmatrix} = \frac{(-1)^{J-M}}{\sqrt{2J+1}}. \quad (63)$$

We will also use the formula (see Eq. 7.35 of [41]³)

³ There is a misprint in the reference.

$$\sum_{\delta\epsilon\phi} (-1)^{d-\delta+e-\epsilon+f-\phi} \begin{pmatrix} d & e & c \\ -\delta & \epsilon & \gamma \end{pmatrix} \begin{pmatrix} e & f & a \\ -\epsilon & \phi & \alpha \end{pmatrix} \begin{pmatrix} f & d & b \\ -\phi & \delta & \beta \end{pmatrix} = \left\{ \begin{matrix} a & b & c \\ d & e & f \end{matrix} \right\} \begin{pmatrix} a & b & c \\ \alpha & \beta & \gamma \end{pmatrix}, \quad (64)$$

where the symbol in curly brackets is a 6-j symbol.

Finally, the Wigner-Eckart theorem for the spherical component q of a rank k tensor reads as⁴ (see [41])

$$\langle \alpha J M | T_q^k | \alpha' J' M' \rangle = \langle \alpha J || \mathbf{T}_k || \alpha' J' \rangle (-1)^{J-M} \begin{pmatrix} J & k & J' \\ -M & q & M' \end{pmatrix}. \quad (65)$$

Now we begin with the proof of Eq. (54). For this case we will drop the index i on the quantum numbers and let $\alpha \neq \alpha'$. On the left hand side of Eq. (54) the addends read as

$$\vec{A}_{i,i} = \langle \alpha J M | \vec{A} | \alpha' J M \rangle = \langle \alpha J || \mathbf{A} || \alpha' J \rangle (-1)^{J-M} \sum_q \begin{pmatrix} J & 1 & J \\ -M & q & M \end{pmatrix} \hat{e}_q, \quad (66)$$

and the corresponding sum over M yields

⁴ Our reduced matrix element contains an extra factor of $\sqrt{2J+1}$ in comparison to that defined in Ref. [41].

$$\begin{aligned}
\sum_M (-1)^{J-M} \begin{pmatrix} J & 1 & J \\ -M & q & M \end{pmatrix} &= \sqrt{2J+1} \sum_M \begin{pmatrix} J & 0 & J \\ -M & 0 & M \end{pmatrix} \begin{pmatrix} J & 1 & J \\ -M & q & M \end{pmatrix}, \\
&= \sqrt{2J+1} \sum_{M,M'} \begin{pmatrix} J & 0 & J \\ -M & 0 & M' \end{pmatrix} \begin{pmatrix} J & 1 & J \\ -M & q & M' \end{pmatrix}, \\
&= 0, \tag{67}
\end{aligned}$$

where we used Eqs. (63), the selection rule $-M + M' = 0$, and the orthogonality of the 3-j symbols. Eqs. (66) and (67) yield the first identity [Eq. (54)].

For the second identity, we can use Eqs. (58) and (65) to write the addends on the left hand side of Eq. (55) as

$$\begin{aligned}
\left(\vec{A}_{i,j} \cdot \vec{u} \right) \vec{A}_{j,i} &= \sum_{q,p} (-1)^q \langle \alpha_i J_i M_i | A_{-q} | \alpha_j J_j M_j \rangle u_q \langle \alpha_j J_j M_j | A_p | \alpha_i J_i M_i \rangle \hat{e}_p, \\
&= \sum_{q,p} (-1)^q \langle \alpha_i J_i || \mathbf{A} || \alpha_j J_j \rangle (-1)^{J_i - M_i} \begin{pmatrix} J_i & 1 & J_j \\ -M_i & -q & M_j \end{pmatrix} u_q \\
&\quad \times \langle \alpha_j J_j || \mathbf{A} || \alpha_i J_i \rangle (-1)^{J_j - M_j} \begin{pmatrix} J_j & 1 & J_i \\ -M_j & p & M_i \end{pmatrix} \hat{e}_p, \tag{68}
\end{aligned}$$

and the corresponding sum over M_i and M_j yields

$$\begin{aligned}
& \sum_{M_i, M_j} (-1)^{J_i - M_i + J_j - M_j} \begin{pmatrix} J_i & 1 & J_j \\ -M_i & -q & M_j \end{pmatrix} \begin{pmatrix} J_j & 1 & J_i \\ -M_j & p & M_i \end{pmatrix} \\
&= \sum_{M_i, M_j} (-1)^{J_i - M_i + J_j - M_j} \begin{pmatrix} J_i & J_j & 1 \\ -M_i & M_j & -q \end{pmatrix} \begin{pmatrix} J_i & J_j & 1 \\ -M_i & M_j & -p \end{pmatrix}, \\
&= (-1)^{-J_i + J_j - q} \sum_{M_i, M_j} \begin{pmatrix} J_i & J_j & 1 \\ -M_i & M_j & -q \end{pmatrix} \begin{pmatrix} J_i & J_j & 1 \\ -M_i & M_j & -p \end{pmatrix}, \\
&= \frac{(-1)^{-J_i + J_j - q}}{\sqrt{3}} \delta_{p, q}, \tag{69}
\end{aligned}$$

where we used the symmetry property for column exchange and for negating all M 's of the 3-j symbol, the selection rule for the M 's to write $M_j = M_i + q$ in the exponent of (-1) , and the fact that $J_i + J_j + 1$ is an integer. Then we replaced $(-1)^{2M_i}$ by $(-1)^{2J_i}$, and used the orthogonality relation of 3-j symbols. Replacing Eqs. (68) and (69) on the left hand side of (55) we get

$$\begin{aligned}
\sum_{M_i, M_j} \left(\vec{A}_{i,j} \cdot \vec{u} \right) \vec{A}_{j,i} &= F \sum_{q,p} u_q \delta_{p,q} \hat{e}_p \\
&= F \vec{u} \tag{70}
\end{aligned}$$

where we defined

$$F \equiv \frac{(-1)^{J_j - J_i}}{\sqrt{3}} |\langle \alpha_i J_i \| \mathbf{A} \| \alpha_j J_j \rangle|^2. \tag{71}$$

Using Eq. (69) with $p = q$, the right hand side of Eq. (55) yields

$$\begin{aligned}
\sum_{M_i, M_j} \left(\vec{A}_{i,j} \cdot \vec{A}_{j,i} \right) &= \sum_{M_i, M_j, q} (-1)^q \langle \alpha_i J_i M_i | A_{-q} | \alpha_j J_j M_j \rangle \langle \alpha_j J_j M_j | A_q | \alpha_i J_i M_i \rangle, \\
&= F \sum_q \delta_{q,q}, \\
&= 3F,
\end{aligned} \tag{72}$$

which in comparison with Eq. (70) yields the identity (55).

For the third identity, we can use Eqs. (58) and (65) to write the addends on the left hand side of Eq. (56) as

$$\begin{aligned}
& \left(\vec{A}_{i,j} \cdot \vec{u} \right) \left(\vec{B}_{k,i} \cdot \vec{v} \right) \vec{C}_{j,k} \\
&= \sum_{p,q,r} (-1)^{p+q} \langle \alpha_i J_i M_i | A_{-p} | \alpha_j J_j M_j \rangle u_p \\
& \quad \times \langle \alpha_k J_k M_k | B_{-q} | \alpha_i J_i M_i \rangle v_q \langle \alpha_j J_j M_j | C_r | \alpha_k J_k M_k \rangle \hat{e}_r, \\
&= \sum_{p,q,r} (-1)^{p+q} \langle \alpha_i J_i || \mathbf{A} || \alpha_j J_j \rangle (-1)^{J_i - M_i} \begin{pmatrix} J_i & 1 & J_j \\ -M_i & -p & M_j \end{pmatrix} u_p \\
& \quad \times \langle \alpha_k J_k || \mathbf{B} || \alpha_i J_i \rangle (-1)^{J_k - M_k} \begin{pmatrix} J_k & 1 & J_i \\ -M_k & -q & M_i \end{pmatrix} v_q \\
& \quad \times \langle \alpha_j J_j || \mathbf{C} || \alpha_k J_k \rangle (-1)^{J_j - M_j} \begin{pmatrix} J_j & 1 & J_k \\ -M_j & r & M_k \end{pmatrix} \hat{e}_r,
\end{aligned} \tag{73}$$

and the corresponding sum over all M_i , M_j , and M_k yields

$$\begin{aligned}
& \sum_{M_i, M_j, M_k} (-1)^{J_i - M_i + J_j - M_j + J_k - M_k} \\
& \times \begin{pmatrix} J_i & 1 & J_j \\ -M_i & -p & M_j \end{pmatrix} \begin{pmatrix} J_k & 1 & J_i \\ -M_k & -q & M_i \end{pmatrix} \begin{pmatrix} J_j & 1 & J_k \\ -M_j & r & M_k \end{pmatrix}, \\
& = (-1)^{2J_i + 2J_j + 2J_k + 3} \sum_{M_i, M_j, M_k} (-1)^{J_i - M_i + J_j - M_j + J_k - M_k} \\
& \times \begin{pmatrix} J_i & J_j & 1 \\ -M_i & M_j & -p \end{pmatrix} \begin{pmatrix} J_j & J_k & 1 \\ -M_j & M_k & r \end{pmatrix} \begin{pmatrix} J_k & J_i & 1 \\ -M_k & M_i & -q \end{pmatrix}, \\
& = (-1)^{2J_k + 1} \left\{ \begin{matrix} 1 & 1 & 1 \\ J_i & J_j & J_k \end{matrix} \right\} \begin{pmatrix} 1 & 1 & 1 \\ r & -q & -p \end{pmatrix}, \\
& = \frac{(-1)^{2J_k + 1}}{\sqrt{6}} \left\{ \begin{matrix} 1 & 1 & 1 \\ J_i & J_j & J_k \end{matrix} \right\} \epsilon_{r, -q, -p}, \tag{74}
\end{aligned}$$

where we used the symmetry property for column exchange of the 3-j symbols, Eqs. (62) and (64), and the fact that $J_i + J_j + 1$ is an integer. Replacing Eqs. (73) and (74) in the left hand side of Eq. (56) and using Eq. (59), we get

$$\begin{aligned}
\sum_{M_i, M_j, M_k} \left(\vec{A}_{i,j} \cdot \vec{u} \right) \left(\vec{B}_{k,i} \cdot \vec{v} \right) \vec{C}_{j,k} &= G \sum_{p,q,r} (-1)^{p+q} u_p v_q \epsilon_{r, -q, -p} \hat{e}_r, \\
&= iG \sum_{p,q,r} (-1)^r i \epsilon_{r,p,q} u_{-p} v_{-q} \hat{e}_r, \\
&= iG \left(\vec{u} \times \vec{v} \right), \tag{75}
\end{aligned}$$

where we defined

$$G \equiv \frac{(-1)^{2J_k+1}}{\sqrt{6}} \langle \alpha_i J_i \| \mathbf{A} \| \alpha_j J_j \rangle \langle \alpha_k J_k \| \mathbf{B} \| \alpha_i J_i \rangle \langle \alpha_j J_j \| \mathbf{C} \| \alpha_k J_k \rangle \begin{Bmatrix} 1 & 1 & 1 \\ J_i & J_j & J_k \end{Bmatrix}. \quad (76)$$

On the right hand side of the identity [Eq. (56)] we have

$$\begin{aligned} (\vec{A}_{i,j} \times \vec{B}_{k,i}) \cdot \vec{C}_{j,k} &= -i \sum_{p,q,r} \epsilon_{pqr} \langle \alpha_i J_i M_i | A_p | \alpha_j J_j M_j \rangle \langle \alpha_k J_k M_k | B_q | \alpha_i J_i M_i \rangle \\ &\quad \times \langle \alpha_j J_j M_j | C_r | \alpha_k J_k M_k \rangle, \\ &= -i \sum_{p,q,r} \epsilon_{pqr} \langle \alpha_i J_i \| \mathbf{A} \| \alpha_j J_j \rangle (-1)^{J_i-M_i} \begin{pmatrix} J_i & 1 & J_j \\ -M_i & p & M_j \end{pmatrix} \\ &\quad \times \langle \alpha_k J_k \| \mathbf{B} \| \alpha_i J_i \rangle (-1)^{J_k-M_k} \begin{pmatrix} J_k & 1 & J_i \\ -M_k & q & M_i \end{pmatrix} \\ &\quad \times \langle \alpha_j J_j \| \mathbf{C} \| \alpha_k J_k \rangle (-1)^{J_j-M_j} \begin{pmatrix} J_j & 1 & J_k \\ -M_j & r & M_k \end{pmatrix}, \end{aligned} \quad (77)$$

and, inverting the sign of q and p in (74), the corresponding sum over M_i , M_j , and M_k yields

$$\begin{aligned} \sum_{M_i, M_j, M_k} (\vec{A}_{i,j} \times \vec{B}_{k,i}) \cdot \vec{C}_{j,k} &= -iG \sum_{p,q,r} \epsilon_{pqr} \epsilon_{rqp}, \\ &= iG \sum_{p,q,r} \epsilon_{pqr}^2, \\ &= 6iG, \end{aligned} \quad (78)$$

which in comparison with Eq. (75) yields Eq. (56).

D. Transition dipoles for chiral electronic states

Opposite enantiomers R and L are related to each other via an inversion, therefore their bound and scattering electronic wave functions satisfy

$$\psi_R(\vec{r}) = \psi_L(-\vec{r}), \quad (79)$$

$$\psi_{\vec{k},R}(\vec{r}) = \psi_{-\vec{k},L}(-\vec{r}). \quad (80)$$

Then, for the transition dipole between two electronic bound states ψ and ψ' we have

$$\begin{aligned} \vec{d}_R &\equiv - \int d\vec{r} \psi_R'^*(\vec{r}) \vec{r} \psi_R(\vec{r}), \\ &= \int d\vec{r} \psi_L'^*(-\vec{r}) (-\vec{r}) \psi_L(-\vec{r}), \\ &= \int d\vec{r} \psi_L'^*(\vec{r}) \vec{r} \psi_L(\vec{r}), \\ &= -\vec{d}_L, \end{aligned} \quad (81)$$

as expected. For the transition dipole between the bound state ψ and the scattering state $\psi_{\vec{k}}$ one has to be more careful because of the vector nature of the photoelectron momentum \vec{k} . In this case we have

$$\begin{aligned} \vec{D}_R(\vec{k}) &= - \int d\vec{r} \psi_{\vec{k},R}^*(\vec{r}) \vec{r} \psi_R(\vec{r}), \\ &= \int d\vec{r} \psi_{-\vec{k},L}^*(-\vec{r}) (-\vec{r}) \psi_L(-\vec{r}), \\ &= \int d\vec{r} \psi_{-\vec{k},L}^*(\vec{r}) \vec{r} \psi_L(\vec{r}), \\ &= -\vec{D}_L(-\vec{k}). \end{aligned} \quad (82)$$

Using Eq. (82) it is a simple matter to confirm that the molecular term in Eq. (13) does indeed have opposite sign for opposite enantiomers:

$$\begin{aligned}
\chi_m^R &= \frac{1}{6} \int d\Omega_k \left[i\vec{D}_R^* (\vec{k}) \times \vec{D}_R (\vec{k}) \right] \cdot \vec{k}, \\
&= \frac{1}{6} \int d\Omega_k \left[i\vec{D}_L^* (-\vec{k}) \times \vec{D}_L (-\vec{k}) \right] \cdot \vec{k}, \\
&= -\frac{1}{6} \int d\Omega_{k'} \left[i\vec{D}_L^* (\vec{k}') \times \vec{D}_L (\vec{k}') \right] \cdot \vec{k}', \\
&= -\chi_m^L,
\end{aligned} \tag{83}$$

where we did the change of variable $\vec{k}' = -\vec{k}$ in the third line.

E. Recovering Ritchie's formula

In Ritchie's original derivation [10] the b_1 factor is given by

$$\begin{aligned}
b_1 &= \left| \tilde{\mathcal{E}} \right|^2 \frac{(4\pi)^2}{3} \sum_{l_j, m_j, \lambda_j, \mu_j, m_1, \mu_1} \left\langle \psi_i \left| r Y_{1\mu_1}^* \right| \psi_{\lambda_j, \mu_j}^{(-)} \right\rangle \left\langle \psi_{l_j m_j}^{(-)} \left| r Y_{1m_1} \right| \psi_i \right\rangle \\
&\times (-1)^{1+m_1+m_j} 3\sqrt{(2l_j+1)(2\lambda_j+1)} \\
&\times \begin{pmatrix} l_j & \lambda_j & 1 \\ 0 & 0 & 0 \end{pmatrix} \begin{pmatrix} 1 & 1 & 1 \\ \sigma & -\sigma & 0 \end{pmatrix} \\
&\begin{pmatrix} l_j & \lambda_j & 1 \\ m_j & -\mu_j & -(m_j - \mu_j) \end{pmatrix} \begin{pmatrix} 1 & 1 & 1 \\ m_1 & -\mu_1 & -(m_1 - \mu_1) \end{pmatrix},
\end{aligned} \tag{84}$$

where the different prefactor in comparison with Eq. (11) in [10] is because we take $W(\vec{k}^L) = \left| \left\langle \psi_{\vec{k}}^{(-)} \left| \hat{e}_\sigma \right| \psi_i \right\rangle \right|^2$ in agreement with Eqs. (3), (5), (7), and (12). If we define

$$D_q^{l_j m_j} \equiv \sqrt{\frac{4\pi}{3}} \langle \psi_{l_j m_j}^{(-)} | r Y_{1q} | \psi_i \rangle, \quad (85)$$

use Eq. (59) for the cross product in spherical components, along with the properties $\epsilon_{pqr} = -\epsilon_{-p, -q, -r}$, $(v_q)^* = (-1)^q (\vec{v}^*)_{-q}$, Eq. (62), and the selection rule $m_1 - \mu_1 - m_j + \mu_j = 0$ of the 3-j symbol, we obtain

$$\begin{aligned} & \sum_{m_1, \mu_1} (-1)^{m_1} \langle \psi_i | r Y_{1\mu_1}^* | \psi_{\lambda_j \mu_j}^{(-)} \rangle \langle \psi_{l_j m_j}^{(-)} | r Y_{1m_1} | \psi_i \rangle \begin{pmatrix} 1 & 1 & 1 \\ m_1 & -\mu_1 & -(m_j - \mu_j) \end{pmatrix}, \\ &= \frac{3}{4\pi} \sum_{m_1, \mu_1} (-1)^{m_1} (D_{\mu_1}^{\lambda_j \mu_j})^* D_{m_1}^{l_j m_j} \begin{pmatrix} 1 & 1 & 1 \\ m_1 & -\mu_1 & -(m_j - \mu_j) \end{pmatrix}, \\ &= \frac{3}{4\pi\sqrt{6}} \sum_{m_1, \mu_1} (-1)^{m_1 - \mu_1} \epsilon_{m_1, -\mu_1, \mu_j - m_j} \left(\vec{D}^{\lambda_j \mu_j *} \right)_{-\mu_1} D_{m_1}^{l_j m_j}, \\ &= -i \frac{1}{4\pi} \sqrt{\frac{3}{2}} (-1)^{m_j - \mu_j} i \sum_{m_1, \mu_1} \epsilon_{m_j - \mu_j, \mu_1, -m_1} \left(\vec{D}^{\lambda_j \mu_j *} \right)_{-\mu_1} D_{m_1}^{l_j m_j}, \\ &= -\frac{1}{4\pi} \sqrt{\frac{3}{2}} \left(i \vec{D}^{\lambda_j \mu_j *} \times \vec{D}^{l_j m_j} \right)_{m_j - \mu_j}. \end{aligned} \quad (86)$$

Then we can use the integral of three spherical harmonics,

$$\begin{aligned} & \int d\Omega_k Y_{l_j, m_j} Y_{\lambda_j, -\mu_j} Y_{1, \mu_j - m_j} \\ &= \sqrt{\frac{3(2l_j + 1)(2\lambda_j + 1)}{4\pi}} \begin{pmatrix} l_j & \lambda_j & 1 \\ 0 & 0 & 0 \end{pmatrix} \begin{pmatrix} l_j & \lambda_j & 1 \\ m_j & -\mu_j & \mu_j - m_j \end{pmatrix}, \end{aligned} \quad (87)$$

equation (58) for the dot product in spherical components, and the selection rule for the sum of the M 's in the 3-j symbol to obtain

$$\begin{aligned}
& -\frac{1}{4\pi} \sqrt{\frac{3}{2}} \sum_{m_j, \mu_j} (-1)^{m_j} \left(i\vec{D}^{\lambda_j \mu_j*} \times \vec{D}^{l_j m_j} \right)_{m_j - \mu_j} \sqrt{(2l_j + 1)(2\lambda_j + 1)} \\
& \times \begin{pmatrix} l_j & \lambda_j & 1 \\ 0 & 0 & 0 \end{pmatrix} \begin{pmatrix} l_j & \lambda_j & 1 \\ m_j & -\mu_j & -(m_j - \mu_j) \end{pmatrix} \\
& = -\frac{1}{4\pi} \sqrt{\frac{3}{2}} \sqrt{\frac{4\pi}{3}} \sum_{m_j, \mu_j} (-1)^{m_j} \left(i\vec{D}^{\lambda_j \mu_j*} \times \vec{D}^{l_j m_j} \right)_{m_j - \mu_j} \int d\Omega_k Y_{l_j, m_j} Y_{\lambda_j, -\mu_j} Y_{1, \mu_j - m_j}, \\
& = -\frac{1}{4\pi} \sqrt{\frac{3}{2}} \sqrt{\frac{4\pi}{3}} \sum_{m_j, \mu_j} (-1)^{m_j - \mu_j} \left(i\vec{D}^{\lambda_j \mu_j*} \times \vec{D}^{l_j m_j} \right)_{m_j - \mu_j} \int d\Omega_k Y_{\lambda_j, \mu_j}^* Y_{l_j, m_j} Y_{1, \mu_j - m_j}, \\
& = -\frac{1}{4\pi} \sqrt{\frac{3}{2}} \sqrt{\frac{4\pi}{3}} \sum_{m_j, \mu_j, q} (-1)^q \left(i\vec{D}^{\lambda_j \mu_j*} \times \vec{D}^{l_j m_j} \right)_q \int d\Omega_k Y_{\lambda_j, \mu_j}^* Y_{l_j, m_j} Y_{1, -q}, \\
& = -\frac{1}{4\pi} \sqrt{\frac{3}{2}} \sum_{m_j, \mu_j} \int d\Omega_k Y_{\lambda_j, \mu_j}^* Y_{l_j, m_j} \left[\left(i\vec{D}^{\lambda_j \mu_j*} \times \vec{D}^{l_j m_j} \right) \cdot \hat{k} \right]. \tag{88}
\end{aligned}$$

Finally, according to Eq. (10) in Ritchie's [10], the scattering wave function is expanded as

$$\psi_{\vec{k}}^{(-)}(\vec{r}) = 4\pi \sum_{l_j, m_j} \psi_{l_j m_j}^{(-)}(\vec{r}) Y_{l_j m_j}^*(\hat{k}) \tag{89}$$

and therefore the dipole transition vector reads as

$$\begin{aligned}
\vec{D} & = \left\langle \psi_{\vec{k}}^{(-)} \left| \vec{d} \right| \psi_i \right\rangle, \\
& = -4\pi \sum_{l_j, m_j, q} \left\langle \psi_{l_j m_j}^{(-)} \left| \sqrt{\frac{4\pi}{3}} r Y_{1, q} \hat{e}_q \right| \psi_i \right\rangle Y_{l_j m_j}(\hat{k}), \\
& = -4\pi \sum_{l_j, m_j} \vec{D}^{l_j m_j} Y_{l_j m_j}(\hat{k}). \tag{90}
\end{aligned}$$

Then, putting together Eqs. (84), (86), (88), and (90), and using Eqs. (13) and (62), we obtain

$$\begin{aligned}
b_1 &= \left| \tilde{\mathcal{E}} \right|^2 (4\pi)^2 \begin{pmatrix} 1 & 1 & 1 \\ \sigma & -\sigma & 0 \end{pmatrix} \frac{1}{4\pi} \sqrt{\frac{3}{2}} \\
&\quad \times \sum_{l_j, m_j, \lambda_j, \mu_j} \int d\Omega_k Y_{\lambda_j, \mu_j}^* Y_{l_j, m_j} \left[\left(i \vec{D}^{\lambda_j \mu_j *} \times \vec{D}^{l_j m_j} \right) \cdot \hat{k} \right] \\
&= \frac{1}{8\pi k} \sigma \left| \tilde{\mathcal{E}} \right|^2 \int d\Omega_k \left[\left(i \vec{D}^* \times \vec{D} \right) \cdot \vec{k} \right] \\
&= \frac{3}{4\pi} \frac{j_z^L}{k}
\end{aligned} \tag{91}$$

which shows that Ritchie's expression for b_1 is equivalent to the one derived here.

F. Circular pump + linear probe

In this appendix we derive Eqs. (36) and (37) from Eqs. (31) and (32) for the case when the pump is circularly polarized according to Eq. (6) and the probe is linearly polarized along \hat{x}^L . From the selection rules already discussed in Sec. IV D we immediately see that the first and last terms in \vec{j}_{diag}^L [Eq. (31)], $\vec{j}_{\text{noncopl}}^L$ [Eq. (33)] and the second term in \vec{j}_{ellip}^L [Eq. (34)] vanish. Furthermore, the remaining terms in \vec{j}_{diag}^L [Eq. (31)] are purely imaginary and also vanish, which only leaves \vec{j}_{lin}^L [Eq. (35)] and the first term in \vec{j}_{ellip}^L [Eq. (34)]. Replacing the field terms in Eq. (34) we obtain

$$\vec{j}_{\text{ellip}}^L(k) = \frac{i\sigma\tilde{\mathcal{E}}}{30} \left(\vec{d}_{0,2}^M \times \vec{d}_{1,0}^M \right) \cdot \int d\Omega_k^M \left[\left(\vec{D}_2^{M*} \cdot \vec{D}_1^M \right) \vec{k}^M \right] e^{i\omega_{21}\tau} \hat{z}^L + \text{c.c.}, \tag{92}$$

whereas for Eq. (35) we obtain

$$\begin{aligned}
\vec{j}_{\text{lin}}^{\text{L}}(k) = & \frac{i\sigma\tilde{\mathcal{E}}}{60} \left\{ \int d\Omega_k^{\text{M}} \left[\left(\vec{d}_{0,2}^{\text{M}} \times \vec{D}_2^{\text{M}*} \right) \cdot \vec{k}^{\text{M}} \right] \left(\vec{d}_{1,0}^{\text{M}} \cdot \vec{D}_1^{\text{M}} \right) \right. \\
& + \int d\Omega_k^{\text{M}} \left[\left(\vec{d}_{0,2}^{\text{M}} \times \vec{D}_1^{\text{M}} \right) \cdot \vec{k}^{\text{M}} \right] \left(\vec{D}_2^{\text{M}*} \cdot \vec{d}_{1,0}^{\text{M}} \right) \\
& + \int d\Omega_k^{\text{M}} \left[\left(\vec{D}_2^{\text{M}*} \times \vec{d}_{1,0}^{\text{M}} \right) \cdot \vec{k}^{\text{M}} \right] \left(\vec{d}_{0,2}^{\text{M}} \cdot \vec{D}_1^{\text{M}} \right) \\
& \left. - \int d\Omega_k^{\text{M}} \left[\left(\vec{d}_{1,0}^{\text{M}} \times \vec{D}_1^{\text{M}} \right) \cdot \vec{k}^{\text{M}} \right] \left(\vec{d}_{0,2}^{\text{M}} \cdot \vec{D}_2^{\text{M}*} \right) \right\} e^{i\omega_{21}\tau\hat{z}^{\text{L}}} \\
& + \text{c.c.}
\end{aligned} \tag{93}$$

where $\tilde{\mathcal{E}} = \tilde{\mathcal{E}}_1^* \tilde{\mathcal{E}}_2^* \tilde{\mathcal{E}}_1 \tilde{\mathcal{E}}_2$. Now, in order to extract $\vec{d}_{0,2}^{\text{M}}$ and $\vec{d}_{1,0}^{\text{M}}$ from the integrals we begin by reordering the expression as

$$\begin{aligned}
\vec{j}_{\text{lin}}^{\text{L}}(k) = & \frac{i\sigma\tilde{\mathcal{E}}}{60} \left\{ \int d\Omega_k^{\text{M}} \left[\left(\vec{D}_2^{\text{M}*} \times \vec{k}^{\text{M}} \right) \cdot \vec{d}_{0,2}^{\text{M}} \right] \left(\vec{D}_1^{\text{M}} \cdot \vec{d}_{1,0}^{\text{M}} \right) \right. \\
& + \int d\Omega_k^{\text{M}} \left[\left(\vec{D}_1^{\text{M}} \times \vec{k}^{\text{M}} \right) \cdot \vec{d}_{0,2}^{\text{M}} \right] \left(\vec{D}_2^{\text{M}*} \cdot \vec{d}_{1,0}^{\text{M}} \right) \\
& - \int d\Omega_k^{\text{M}} \left[\left(\vec{D}_2^{\text{M}*} \times \vec{k}^{\text{M}} \right) \cdot \vec{d}_{1,0}^{\text{M}} \right] \left(\vec{D}_1^{\text{M}} \cdot \vec{d}_{0,2}^{\text{M}} \right) \\
& \left. - \int d\Omega_k^{\text{M}} \left[\left(\vec{D}_1^{\text{M}} \times \vec{k}^{\text{M}} \right) \cdot \vec{d}_{1,0}^{\text{M}} \right] \left(\vec{D}_2^{\text{M}*} \cdot \vec{d}_{0,2}^{\text{M}} \right) \right\} e^{i\omega_{21}\tau\hat{z}^{\text{L}}} \\
& + \text{c.c.},
\end{aligned} \tag{94}$$

to apply the vector identity $(\vec{a} \cdot \vec{c})(\vec{b} \cdot \vec{d}) - (\vec{a} \cdot \vec{d})(\vec{b} \cdot \vec{c}) = (\vec{a} \times \vec{b}) \cdot (\vec{c} \times \vec{d})$, which yields

$$\begin{aligned}
\vec{j}_{\text{lin}}^{\text{L}}(k) = & \frac{i\sigma\tilde{\mathcal{E}}}{60} \left(\vec{d}_{0,2}^{\text{M}} \times \vec{d}_{1,0}^{\text{M}} \right) \cdot \left\{ \int d\Omega_k^{\text{M}} \left[\left(\vec{D}_2^{\text{M}*} \times \vec{k}^{\text{M}} \right) \times \vec{D}_1^{\text{M}} \right] \right. \\
& + \int d\Omega_k^{\text{M}} \left[\left(\vec{D}_1^{\text{M}} \times \vec{k}^{\text{M}} \right) \times \vec{D}_2^{\text{M}*} \right] \left. \right\} e^{i\omega_{21}\tau} \hat{z}^{\text{L}} \\
& + \text{c.c.}
\end{aligned} \tag{95}$$

Now we use the vector identity $(\vec{a} \times \vec{b}) \times \vec{c} = (\vec{a} \cdot \vec{c})\vec{b} - (\vec{b} \cdot \vec{c})\vec{a}$ to get

$$\begin{aligned}
\vec{j}_{\text{lin}}^{\text{L}}(k) = & \frac{i\sigma\tilde{\mathcal{E}}}{60} \left(\vec{d}_{0,2}^{\text{M}} \times \vec{d}_{1,0}^{\text{M}} \right) \int d\Omega_k^{\text{M}} \left\{ 2 \left(\vec{D}_2^{\text{M}*} \cdot \vec{D}_1^{\text{M}} \right) \vec{k}^{\text{M}} - \left(\vec{k}^{\text{M}} \cdot \vec{D}_1^{\text{M}} \right) \vec{D}_2^{\text{M}*} \right. \\
& \left. - \left(\vec{k}^{\text{M}} \cdot \vec{D}_2^{\text{M}*} \right) \vec{D}_1^{\text{M}} \right\} e^{i\omega_{21}\tau} \hat{z}^{\text{L}} + \text{c.c.}
\end{aligned} \tag{96}$$

Adding Eqs. (92) and (96) yields Eqs. (36) and (37).

-
- [1] U. Boesl and A. Kartouzian, *Annual Review of Analytical Chemistry* **9**, 343 (2016).
 - [2] M. H. Janssen and I. Powis, *Spectroscopy* **15**, 16 (2017).
 - [3] G.-Q. Lin, Q.-D. You, and J.-F. Cheng, *Chiral Drugs: Chemistry and Biological Action* (Wiley, 2011).
 - [4] R. Cireasa, A. E. Boguslavskiy, B. Pons, M. C. H. Wong, D. Descamps, S. Petit, H. Ruf, N. Thiré, A. Ferré, J. Suarez, J. Higuët, B. E. Schmidt, A. F. Alharbi, F. Légaré, V. Blanchet, B. Fabre, S. Patchkovskii, O. Smirnova, Y. Mairesse, and V. R. Bhardwaj, *Nature Physics* **11**, 654 (2015).
 - [5] O. Smirnova, Y. Mairesse, and S. Patchkovskii, *Journal of Physics B: Atomic, Molecular and Optical Physics* **48**, 234005 (2015).

- [6] D. Ayuso, P. Decleva, S. Patchkovskii, and O. Smirnova, *Journal of Physics B: Atomic, Molecular and Optical Physics* **51**, 06LT01 (2018).
- [7] D. Ayuso, P. Decleva, S. Patchkovskii, and O. Smirnova, *Journal of Physics B: Atomic, Molecular and Optical Physics* **51**, 124002 (2018).
- [8] Y. Zhang, J. R. Rouxel, J. Autschbach, N. Govind, and S. Mukamel, *Chem. Sci.* **8**, 5969 (2017).
- [9] J. R. Rouxel, M. Kowalewski, and S. Mukamel, *Structural Dynamics* **4**, 044006 (2017).
- [10] B. Ritchie, *Physical Review A* **13**, 1411 (1976).
- [11] N. Cherepkov, *Chemical Physics Letters* **87**, 344 (1982).
- [12] I. Powis, *The Journal of Chemical Physics* **112**, 301 (2000).
- [13] N. Böwering, T. Lischke, B. Schmidtke, N. Müller, T. Khalil, and U. Heinzmann, *Physical Review Letters* **86**, 1187 (2001).
- [14] P. Fischer, D. S. Wiersma, R. Righini, B. Champagne, and A. D. Buckingham, *Physical Review Letters* **85**, 4253 (2000).
- [15] P. Fischer, A. D. Buckingham, and A. C. Albrecht, *Phys. Rev. A* **64**, 053816 (2001).
- [16] D. Patterson, M. Schnell, and J. M. Doyle, *Nature* **497**, 475 (2013).
- [17] A. Yachmenev and S. N. Yurchenko, *Phys. Rev. Lett.* **117**, 033001 (2016).
- [18] S. Beaulieu, A. Comby, D. Descamps, B. Fabre, G. A. Garcia, R. Geneaux, A. G. Harvey, F. Legare, Z. Masin, L. Nahon, A. F. Ordonez, S. Petit, B. Pons, Y. Mairesse, O. Smirnova, and V. Blanchet, *arXiv:1612.08764 [physics]* (2016), arXiv: 1612.08764; S. Beaulieu, A. Comby, D. Descamps, B. Fabre, G. A. Garcia, R. G eneaux, A. G. Harvey, F. L egar e, Z. Mas ın, L. Nahon, A. F. Ordonez, S. Petit, B. Pons, Y. Mairesse, O. Smirnova, and V. Blanchet, *Nature Physics* **14**, 484 (2018).
- [19] D. Patterson and J. M. Doyle, *Physical Review Letters* **111**, 023008 (2013).
- [20] K. K. Lehman, *Frontiers and Advances in Molecular Spectroscopy, Chapter 21: Theory of Enantiomer-Specific Microwave Spectroscopy*, 1st ed., edited by J. Laane (Elsevier,

2018).

- [21] C. Lux, M. Wollenhaupt, T. Bolze, Q. Liang, J. Koehler, C. Sarpe, and T. Baumert, *Angewandte Chemie International Edition* **51**, 5001 (2012).
- [22] C. S. Lehmann, R. B. Ram, I. Powis, and M. H. M. Janssen, *The Journal of Chemical Physics* **139**, 234307 (2013).
- [23] C. Lux, M. Wollenhaupt, C. Sarpe, and T. Baumert, *ChemPhysChem* **16**, 115 (2015).
- [24] S. Beaulieu, A. Ferre, R. Geneaux, R. Canonge, D. Descamps, B. Fabre, N. Fedorov, F. Legare, S. Petit, T. Ruchon, V. Blanchet, Y. Mairesse, and B. Pons, *New Journal of Physics* **18**, 102002 (2016).
- [25] I. Dreissigacker and M. Lein, *Phys. Rev. A* **89**, 053406 (2014).
- [26] I. Powis, *The Journal of Chemical Physics* **112**, 301 (2000).
- [27] V. Ulrich, S. Barth, S. Joshi, U. Hergenhahn, E. Mikajlo, C. J. Harding, and I. Powis, *The Journal of Physical Chemistry A* **112**, 3544 (2008).
- [28] L. Nahon, G. A. Garcia, C. J. Harding, E. Mikajlo, and I. Powis, *The Journal of Chemical Physics* **125**, 114309 (2006).
- [29] L. Nahon, G. A. Garcia, and I. Powis, *Journal of Electron Spectroscopy and Related Phenomena Gas phase spectroscopic and dynamical studies at Free-Electron Lasers and other short wavelength sources*, **204, Part B**, 322 (2015).
- [30] L. Nahon, L. Nag, G. A. Garcia, I. Myrgorodska, U. Meierhenrich, S. Beaulieu, V. Wanie, V. Blanchet, R. Geneaux, and I. Powis, *Phys. Chem. Chem. Phys.* **18**, 12696 (2016).
- [31] M. M. R. Fanood, N. B. Ram, C. S. Lehmann, I. Powis, and M. H. M. Janssen, *Nature Communications* **6**, 7511 (2015).
- [32] M. M. R. Fanood, M. H. M. Janssen, and I. Powis, *The Journal of Chemical Physics* **145**, 124320 (2016).
- [33] R. E. Goetz, T. A. Isaev, B. Nikoobakht, R. Berger, and C. P. Koch, *The Journal of*

- Chemical Physics **146**, 024306 (2017).
- [34] N. Manakov, S. Marmo, and A. Meremianin, Journal of Physics B: Atomic, Molecular and Optical Physics **29**, 2711 (1996).
 - [35] M. Y. Agre, Optics and spectroscopy **101**, 356 (2006).
 - [36] I. Tinoco, The Journal of Chemical Physics **62**, 1006 (1975), <https://doi.org/10.1063/1.430566>.
 - [37] J. A. Giordmaine, Physical Review **138**, A1599 (1965).
 - [38] H. W. Kroto, *Molecular Rotation Spectra*, Dover Books on Physics and Chemistry (Dover Publications, 1992).
 - [39] L. D. Barron, *Molecular light scattering and optical activity*, 2nd ed. (Cambridge University Press, Cambridge, UK ; New York, 2004).
 - [40] D. L. Andrews and T. Thirunamachandran, The Journal of Chemical Physics **67**, 5026 (1977).
 - [41] D. M. Brink and G. R. Satchler, *Angular Momentum*, 2nd ed. (Clarendon Press, Oxford, 1968).